AFOSR Scientific Report
AFOSR-69-1425TR

Contract No. AF 49(638)-1623
Project No. 9781-01

EXPERIMENTAL MEASUREMENTS OF HYPERSONIC CORNER FLOW

by

Charles T. Narcho and Robert J. Cresci

JANUARY 1969

POLYTECHNIC INSTITUTE OF BROOKLYN

DEPARTMENT
of
AEROSPACE ENGINEERING
and
APPLIED MECHANICS

PIBAL REPORT No. 1069

AFOSR Scientific Report
AFOSR-69-1228TR

EXPERIMENTAL MEASUREMENTS OF HYPERSONIC CORNER FLOW

by

Charles T. Nardo and Robert J. Cresci

This research was supported by the Air Force Office of Scientific Research under Contract No. AF 49(638)-1623, Project No. 9781-01.

Polytechnic Institute of Brooklyn

Department

of

Aerospace Engineering and Applied Mechanics

January 1969

PIBAL Report No. 69-1

EXPERIMENTAL MEASUREMENTS OF HYPERSONIC CORNER FLOW[†]

by

Charles T. Nardo[*] and Robert J. Cresci[**]
Polytechnic Institute of Brooklyn

ABSTRACT

An experimental investigation has been conducted of the viscous-inviscid interaction occurring along the interior corner of two intersecting flat plates under hypersonic, low density, conditions.

The program involves the measurement of surface heat transfer rates and surface pressures in the vicinity of a corner with included angles of 60°, 90° and 120°. The interpretation of these measurements gives rise to some understanding of local flow behavior and, therefore, on the nature of the three-dimensional boundary layer and shock shape within the corner region. In addition, pitot and temperature surveys are conducted in cross planes to obtain information pertaining to the flow field variables within the corner region, and also, the complex shock

---

[†] This research was supported by the Air Force Office of Scientific Research under Contract No. AF 49(638)-1623, Project No. 9781-01.

Special thanks are due to the National Aeronautics and Space Administration for support given under the NASA Predoctoral Traineeship Program.

[*] NASA Trainee

[**] Professor of Aerospace Engineering and Assistant Director of Gas Dynamics Laboratory

TABLE OF CONTENTS

LIST OF ILLUSTRATIONS

LIST OF SYMBOLS

C	=	$T_{\infty}\mu/T\mu_{\infty}$ - Chapman - Rubesin Constant
C_f	=	$2\tau_w/\rho_{\infty} u_{\infty}^2$ - skin friction coefficient
H		stagnation enthalpy
k		coefficient of thermal conductivity
M		Mach number
p		pressure
q	=	$(k \partial T/\partial y)$ - heat transfer rate
Re_x	=	$\rho ux/\mu$ - Reynolds number
S_t	=	$q_w/\rho_{\infty} u_{\infty} (H_{\infty} - H_w)$ - Stanton number
T		temperature
u		velocity in the streamwise direction
x		coordinate in the streamwise direction
y		coordinate normal to x axis and z axis
z		coordinate along horizontal surface normal to x axis
δ		boundary layer thickness
ν		interior corner angle
ρ		mass density
τ	=	$(\mu \partial u / \partial y)$ - shear stress
μ		coefficient of viscosity
$\bar{\chi}$	=	$M_{\infty}^3 \sqrt{C/Re_{x_{\infty}}}$ - Viscous-Inviscid interaction parameter

Subscripts

e	conditions external to boundary layer
s	stagnation conditions
w	conditions calculated at the surface

$z \to \infty$, 2-D	flat plate conditions
∞	free stream conditions
2	conditions behind a normal shock

I. INTRODUCTION

The three-dimensional, low density, hypersonic flow occurring in the interior corner of two intersecting flat plates represents a basic flow configuration of significant interest to both experimental and theoretical aerodynamicists. This particular flow configuration has practical applicability in relation to lifting and control surfaces and wing-body intersections of hypersonic flight vehicles at high altitudes. Due to its current interest, a considerable amount of effort has been devoted toward solving the complicated flow system within the region of corner influence.

The inviscid flow field generated by corner intersections has been studied quite extensively in its supersonic counterpart, cf. references (1) through (4), however, the basic mechanism of interaction in hypersonic flow is quite different. In the supersonic case, the interaction occurs by virtue of the convergence of the two-dimensional flows generated over each planar wedge surface. In the hypersonic case, however, the interaction takes place due to the viscous-inviscid interaction produced, since the shock layer and the boundary layer are of the same order of magnitude under these conditions. Therefore, one can no longer treat the boundary layer problem and the shock layer problem independently since the two layers are intimately coupled. These coupling effects have made the theoretical treatment of this problem very difficult until quite recently. Even with the development of the analyses of ref. (5) - (7), moreover, experimental data is required under a wide variety of conditions to verify these analyses for the different flow regimes of interest.

In addition, detailed flow field measurements are always necessary in the determination of new techniques for improving existing analyses.

The viscous layer in a rectangular corner has been studied experimentally in the weak interaction regime ($\overline{\chi} < 1$) in reference (8) and in the strong interaction regime in reference (9). The latter research program was extended in reference (10) to include the inviscid flow field and also to determine the shock configuration in the vicinity of the corner. The bifurcated shock configuration which results is qualitatively similar to that achieved in reference (4) in which there was negligible viscous interaction. This complex shock shape has yet to be verified analytically.

The current study presents an experimental investigation of the low density, hypersonic flow in a non-rectangular corner formed by two sharp, flat plates whose intersection line lies parallel to the free stream velocity. Primary emphasis in this paper is placed on the measurement of surface heat transfer rates, surface pressures, and some flow field characteristics in the viscous and shock layers. The tests were conducted at a free stream Mach number of 11.2 at a Reynolds number of 1.5×10^4/in. The flow field surveys were conducted in planes perpendicular to the free stream at values of the hypersonic interaction parameter ($\overline{\chi} = M_\infty{}^3 \sqrt{C/Re_{x_\infty}}$) of 2.5 and 5.0. The surface measurements correspond to values of $\overline{\chi}$ between 1.5 and 17. Effects of varying the interior corner angle between 60°, 90°, and 120° were also investigated.

Some results of the initial experimental programs in rectangular corners were reported in references (9) and (10) in which measurements

of heat transfer and pressure were presented over a range of $\overline{\chi}$ of 1.0 through 17. The present paper presents an extension of these initial investigations in order to give a more complete picture of the entire corner region (i.e., both viscous and inviscid layers), and, in addition, to study the effects of non-rectangular corner geometries. The previous data are compared with the measurements obtained in the present program to provide a general picture of the effects of varying corner geometry.

II. MODEL DESIGN AND TEST PROCEDURES

The test model under consideration consists of two sharp flat plates intersecting along a line parallel to the free stream, cf., fig. (1). The leading edges of both plates are unswept and are machined to a nose radius of less than 0.001 inches. The interior corner angle is adjustable to study the effect of corner geometry on the flow field pattern within the corner region. The three angles utilized in this program are 60°, 90°, and 120°. A schematic of the model along with its internal instrumentation details is shown in figure (1). This entire configuration is sting mounted in the Mach 11.2 blow down test facility (see figure 2) of the Gas Dynamics Research Laboratory of PIB.

To measure surface static pressures, thermal conductivity type Hastings gauges are used, since in the range of static pressures measured, namely 100-1000 microns, these transducers proved to be the most accurate. The Hastings gauges are inserted directly beneath the surface of the plate with a 1/16 inch diameter exposed pressure orifice to achieve rapid response time. Surface heat transfer data is obtained from circular, stainless steel, shim-stock disks which are inserted flush with the plate surface; 40 gauge Chromel-Alumel thermocouple wires are spotwelded to the underside of the disks. The heat transfer rate is therefore proportional to the rate of change of temperature with time; the constant of proportionality being related to the thickness and density of the stainless disk. All instrumentation cables are located

within the sting mount and passed through the tunnel wall through vacuum fittings. The test data is recorded on Honeywell and Bristol strip chart recorders and analyzed directly from these permanent traces.

During the course of the experimental investigation, two types of flow field survey rakes are used at the two cross planes of interest. Rake No. 1 is used in the cross plane equivalent to $\bar{\chi} = 2.5$; this particular rake contained two stagnation pressure probes, cf. figure (2), of 1/16 inch outside diameter. For a constant value of z, obtained by adjusting the vertical plate with respect to the probe centerline, variations in the y coordinate are obtained through the use of a gear and pinion device manipulated external to the tunnel. In this manner, the tunnel pressure is maintained on the order of a few millimeters of Hg between tests which increases the testing frequency. To record pitot pressures, variable reluctance transducers are used since the pitot pressure level is somewhat higher than the surface pressures. The particular transducers used have a range of 2-40 millimeters of Hg. Total temperature probes are also used on the same rake after completion of the pressure tests. These probes are of the open tip variety, constructed from 40 gauge Cromel-Alumel wire with a distance of 0.30 inches between end supports. This configuration was found to give minimal end support interference and relatively fast response times.

Rake No. 2 is used to examine the flow characteristics in a cross-plane corresponding to $\bar{\chi} = 5.0$ (see figure 2). This seemingly complex configuration is necessary for probe rigidity and to

minimize the rake support interference. Both pitot and total temperature probes are inserted in this rake on alternate test series. It is found that 1/16 inch diameter tubing is sufficiently large to give fast response times and negligible viscous effects, yet small enough to give an accurate location of the shock position (as determined by a region of rapidly varying pitot pressure).

The overall accuracy of the data obtained is established by instrumentation accuracy and repeatability of test data. The temperature data is believed to be within $\pm$ 5 % of its true value. No effort was made to correct the temperature data for the actual recovery temperature since the experimental scatter exceeds this correction and, in addition, all temperatures are normalized with respect to the free stream stagnation temperature. This reduces the errors introduced by omitting the correction due to the recovery factor. The pressure data is accurate to within $\pm$ 10 %. It should be noted that Statham strain gauge transducers are used in regions where the stagnation pressure is expected to exceed the upper limits of accuracy of the reluctance transducers. Where the range of validity of the pressure transducers overlapped, readings from both types are used to determine repeatability and overall accuracy.

The horizontal plate is aligned to within $\pm$ 10 min. of angular deflection in the tunnel, however, the vertical plate presented some difficulty in this connection. Alignment is performed mechanically with respect to the tunnel walls, and then checked aerodynamically by examining the symmetry of the data obtained on both surfaces.

It may be noted that in the 60° configuration, a 10 % error results in the shock displacement distance from the fin surface. Both the 90° and 120° corners, however, produce errors less than 4 %. Even for the 60° configuration, moreover, this inaccuracy is not sufficient to alter the general flow field characteristics within the corner envelope of interest.

The test procedure is carried out as follows:

(i) Check calibrations of all pressure transducers are obtained during the tunnel pump down phase, and compared to the calibration curves obtained before the test.

(ii) The pebble bed heater is then pressurized, the throat valve withdrawn, and the tunnel started. Test times of 3-4 seconds proved sufficiently long so that both pressure and temperature measurements achieved steady state values.

(iii) Following each test, the tunnel test section is allowed to reach a steady state condition and an additional calibration check is taken; the tunnel is then pumped down for the next test.

III. PRESENTATION AND DISCUSSION OF EXPERIMENTAL DATA

The initial portion of this experimental program was devoted toward the study of the two-dimensional flow field characteristics corresponding to large lateral distances from the corner. Data pertaining to flat plate overpressures, Stanton number, and skin friction coefficient were reported and compared to available theoretical analyses in reference (9) consequently, these data will not be repeated here.

In addition to the pitot pressures and stagnation temperatures measured within the corner layer, one is also interested in obtaining the static pressure to determine local Mach no., velocity, etc. Unfortunately, due to the flow angularity and viscous interference on the static probe, this information was not attainable in this test program.

The surface static pressures, however, were obtained and are shown in figure (3) for $\bar{\chi} = 5.0$. It is noted that the data peaks at some distance away from the corner and then asymptotes to the local two-dimensional value far from the region of corner influence. The two-dimensional theoretical values are obtained from ref. (11) and (12). As the corner angle decreases, the peak moves away from the corner and increases in magnitude. For the 120° configuration, little overshoot is observed in the surface pressure.

The surface heating rates are presented in figures (4a) through (4d) as a function of distance from the corner, for various values of $\bar{\chi}$ and included corner angles. Similar data were obtained in refer-

ence (9) for the 90° configuration which is included here for comparison. The typical behavior can be observed in figure (4a); the heat transfer increases from zero at the corner to a peak value above that of a two-dimensional flat plate and then decreases to the flat plate value far from the corner. For the smaller included angles, higher peak heating rates result and, in addition, the location of the peak occurs further from the corner. This is consistent with the behavior of the surface pressure data where the corner region of disturbance is also more extensive for the smaller included angle. The location of the peak value of Stanton number with respect to the local two-dimensional boundary layer thickness is noted in figure (4) where the boundary layer thickness for an infinite plate is included corresponding to each value of $\bar{\chi}$. The peak seems to occur approximately at a distance equal to the two-dimensional boundary layer thickness from the corner. The peak is further from the corner for $\eta = 60^{\circ}$ and slightly closer for $\eta = 120^{\circ}$; in fact, the location of the maximum heating appears to closely correspond to the projection of intersection of the undisturbed two-dimensional boundary layer edges on each surface.

The peak heating rates in terms of the maximum Stanton number are shown in figure (5) as a function of $\bar{\chi}$ including the data of reference (9) and the lower Mach number ($M_{\infty} = 8.0$) data of reference (13). As $\bar{\chi}$ decreases (in the downstream direction) the peak value decreases and its location also moves away from the corner. As the included angle increases, the overall heat transfer approaches

that of a two-dimensional plate with only an extremely small region of low heat transfer into the immediate corner region. The zero interaction, boundary layer analysis of reference (14) is also shown in this figure for comparison. It can be observed that two different theoretical curves result from this analysis for the two sets of data obtained at different free stream Mach numbers. This occurs since the heat transfer parameter that correlates with the viscous interaction parameter ($\bar{\chi}$) is $M_\infty^3 S_t$ rather than the Stanton number alone if there is no viscous interaction. In either case, the two-dimensional data agrees quite well with the boundary layer theory for low $\bar{\chi}$. The experimental data for the 60° and 90° angles, however, appear to correlate directly in terms of S_t for both sets of data, indicating that the peak heating is dominated more by the three-dimensional, strong interaction effects in the corner than by usual boundary layer behavior even at lower values of $\bar{\chi}$.

Typical pitot pressure profiles are shown in figures (6a) through (6i) for both the 60° and 90° corners at $\bar{\chi} = 5.0$. The value indicated for the "y" coordinate is measured from the fin surface; therefore, for the 60° corner, constant values of "z" do not correspond to a profile normal to the plate but to one inclined at 60° to the surface. Fig. (6i) shows the complete two-dimensional profile far from the corner correspondly to a completely two-dimensional flow ($y = 90^\circ$). Since the data for $= 60^\circ$, along a line of constant "y", does not correspond to a profile normal to the fin surface, this data was plotted as a function of the actual normal coordinate (z sin) to facilitate comparison between the two profiles. It is observed, as noted previously,

that the two-dimensional shock location on the fin for the 60° corner is slightly less than for the 90° corner; this is due to a slight misalignment of the fin.

From the surface static pressure distribution of figure (3) and the pitot pressures close to the wall, the local skin friction coefficient can be obtained. These data are shown in figure (7) for $\omega = 60^{\circ}$ and $\omega = 90^{\circ}$, at $\bar{\chi} = 5.0$; skin friction coefficient times the square root of Reynolds number is plotted versus the distance from the corner. It is observed that the magnitude of the peak does not change significantly, however, the distribution does. For the smaller corner angle, the peak skin friction moves outward and exhibits a somewhat slower decay to the local two-dimensional value.

The location of the imbedded shocks can be determined quite accurately from the pitot pressure plots as the region where a "discontinuity" in pitot pressure results; this "discontinuity" is smeared slightly due to the finite probe diameter. In figure (6e), for example, the $\omega = 90^{\circ}$ configuration indicates a strong shock wave at $z = 1.15$ inches and a weaker wave at $z = 1.05$ inches. Comparison of the data for the two different corner angles shows a distinct difference in the flow behavior. For the 60° angle, the shock waves are significantly stronger as characterized by the greater jump in pitot pressure across them. Due to the complicated nature of the flow in the corner, it is difficult to establish the overall shock pattern and general flow behavior from these plots. One can get a better picture of the entire flow pattern if one examines, for example, a

cross section of the corner region including contours of constant pitot pressures. This is shown in figure (8) for both corner angles at $\bar{\chi} = 5$. The differences in the shock pattern for the two corner angles is made more obvious in these plots. For the 90° corner, the bifurcated shock in the corner intersects the two-dimensional shock and appears to generate two additional shock waves at each end; one approaches the plane of symmetry and is rapidly attenuated while the other approaches the plate surface and extends into the boundary layer. In the 60° configuration, however, the extent of the bifurcated shock is decreased considerably and generates only one additional shock at its point of intersection with the two-dimensional shock wave. This shock also extends into the boundary layer and is considerably stronger than in the 90° case. The two pitot pressure peaks existing in the 90° corner have also degenerated into one peak (of larger magnitude) in the 60° corner region.

Stagnation temperature profiles were also obtained and are shown in figures (9a) through (9d) for $\omega = 60^{\circ}$ and 90° and at $\bar{\chi} = 5.0$. The region of corner influence on the stagnation temperature is considerably smaller than either on the pitot pressure or on the heat transfer since here the variation is confined completely to the viscous layer. The behavior in this case is quite similar to that obtained in the 90° corner at $\bar{\chi} = 2.5$, cf. reference (9), where a high temperature core occurred in the immediate vicinity of the corner. Again, to facilitate the ease with which one may interpret the data, stagnation tempeature contours in the 60° and 90° corner for $\bar{\chi} = 5.0$ have been plotted and are shown in figures (10a) and (10b).

IV. CONCLUSIONS

An experimental investigation of the hypersonic interaction flow along the interior corner of two intersecting flat plates has been presented. From these results, once can draw several major conclusions. (i) The surface measurements of pressure and heating rates indicate a region of high pressure and high heat transfer in the immediate vicinity of the corner. Moreover, the ratio of local peak values to the value far from the corner increases with downstream distance (decreasing $\bar{\chi}$). (ii) Although the skin friction coefficient decreases to zero as one approaches the corner, the extremely high overshoot in the immediate vicinity of the corner results in integrated values of skin friction which increase the total drag coefficient of the corner configuration. (iii) The effect of decreasing the corner interior angle results in a larger envelope of corner disturbance and higher overshoots of surface pressure, heat transfer, and skin friction thereby discouraging design configurations including this type of surface intersection.

V. REFERENCES

1. Wallace J. and Clark, J. H.: "Uniformly Valid Second-Order Solution for Supersonic Flow Over Cruciform Surfaces," AIAA Journal, Vol. 1, No. 1, pp. 179-185, January 1963.

2. Hains, F. D.: "Supersonic Flow Near the Junction of Two Wedges" Jour. Aerospace Sci., Vol. 25, No. 8, pp. 530-531, August 1958.

3. Stainback, P. Calvin: "An Experimental Investigation at a Mach Number of 2.95 of Flow in the Vicinity of a 90° Interior Corner Aligned With the Free-Stream Velocity." NASA TN D-184, February 1960.

4. Charwat, A. F., and Redekopp, L. G.: "Supersonic Interference Flow Along the Corner of Intersecting Wedges". AIAA Journal, Vol. 5, No. 3, pp. 480-488, March 1967.

5. Rudman, S. and Rubin, S. G.: "Hypersonic Viscous Flow Over Slender Bodies Having Sharp Leading Edges". AIAA Journal, Vol. 6, No. 10, pp. 1883-1889, October 1968.

6. Cresci, R. J., Rubin, S. G., and Nardo, C. T.: "Hypersonic Flow in Rectangular and Non-Rectangular Corners." Paper presented at the AGARD Specialists' Meeting on Hypersonic Boundary Layers and Flow Fields, held at Royal Aeronautical Society, London, England, May 1968, AGARD CP No. 30.

7. Rubin, S. G., Lin, T. C., Pierucci, M., and Rudman, S.: "Hypersonic Interactions Near Sharp Leading Edges". PIBAL

Report No. 68-17, AFOSR 68-1368, June 1968; also, "Hypersonic Viscous-Inviscid Interaction by a New Type of Analysis", pres. at the AGARD Specialists' Meeting on Hypersonic Boundary Layers and Flow Fields, Royal Aeronautical Society, London, England, May 1968, AGARD CP No. 30.

8. Stainback, P. Calvin: "Heat-Transfer Measurements at a Mach Number of 8 in the Vicinity of a 90^{o} Interior Corner Aligned with the Free-Stream Velocity." NASA TN D-2417, August 1964.

9. Cresci, R. J.: "Hypersonic Flow Along Two Intersecting Planes". PIBAL Report No. 895, March 1966; also, Proc. of the 1966 Heat Transfer and Fluid Mechanics Institute, University of Santa Clara, California, June 22-24, 1966. Stanford Univ. Press, Ed. by M. A. Saad and J. A. Miller, 1966.

10. Nardo, C. T.: "Hypersonic Interaction Effects Along the Interior Corner of Two Intersecting Flat Plates", Master Thesis, Polytechnic Institute of Brooklyn, June 1967.

11. Lees, L. and Probstein, R. F.: "Hypersonic Viscous Flow Over a Flat Plate". Report No. 195 (Contract AF 33(038)-250) Aero. Eng. Lab., Princeton University, April 1952.

12. Bertram, M. H. and Blackstock, T. A.: "Some Simple Solutions to the Problem of Predicting Boundary Layer Self-Induced Pressures". NASA TN D-798, April 1961.

13. Stainback, P. C. and Weinstein, L. M.: "Aerodynamic Heating in the Vicinity of Corners at Hypersonic Speeds". NASA TN D-4130, November 1967.

14. Eckert, E. R. G.: "Survey on Heat Transfer at High Speeds", Wright Air Development Center, TR 54-70, 1954.

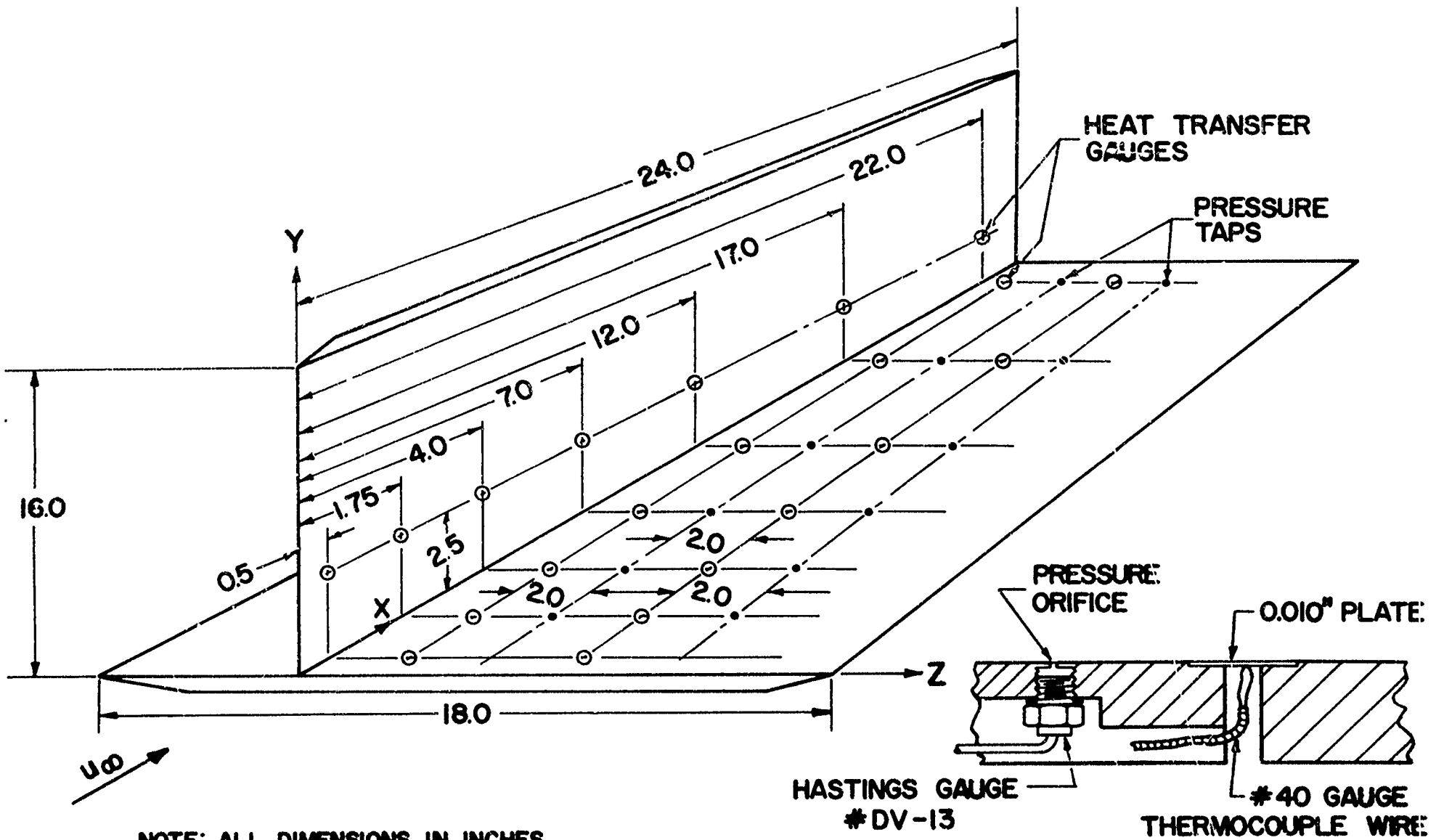

NOTE: ALL DIMENSIONS IN INCHES.

FIG. (1) MODEL DESIGN AND INSTRUMENTATION DETAILS.

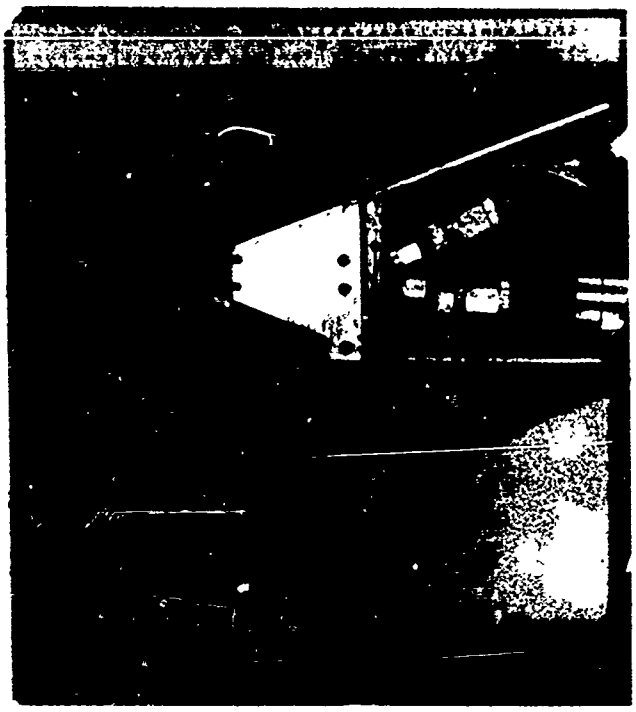

Rake # 1

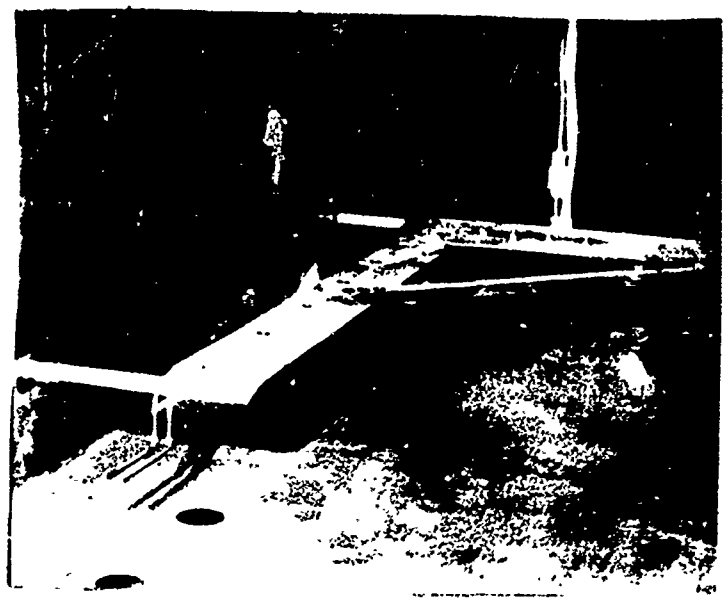

Rake #2

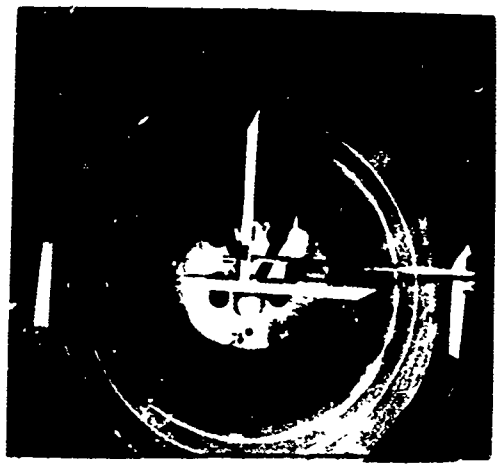

Sting Mounted Model in Mach 11.2 Tunnel

FIG. (2) PHOTOGRAPHS OF MODEL AND SURVEY RAKES

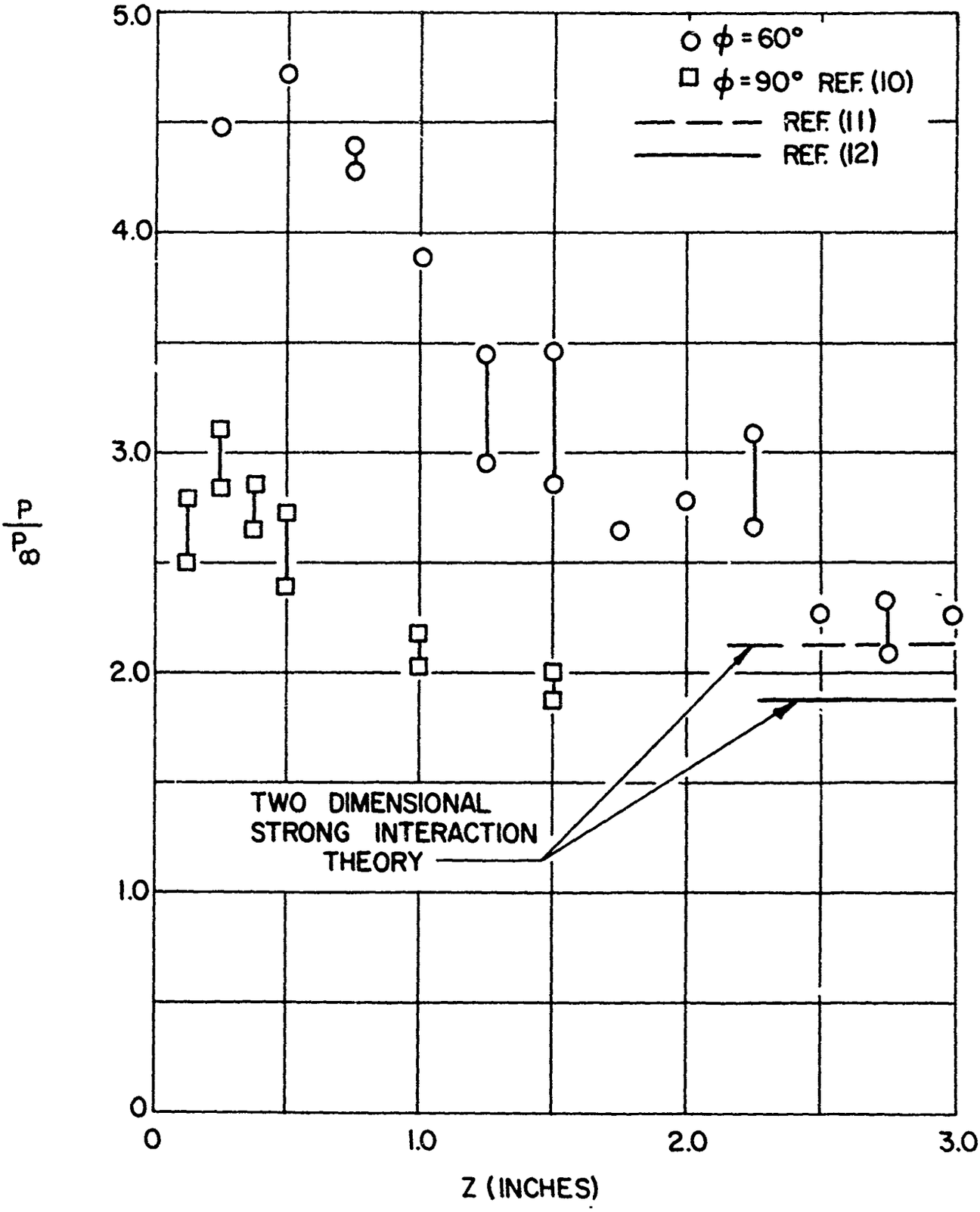

FIG. (3) STATIC PRESSURE DISTRIBUTION IN CORNER REGION – $\bar{X}$ = 5.0

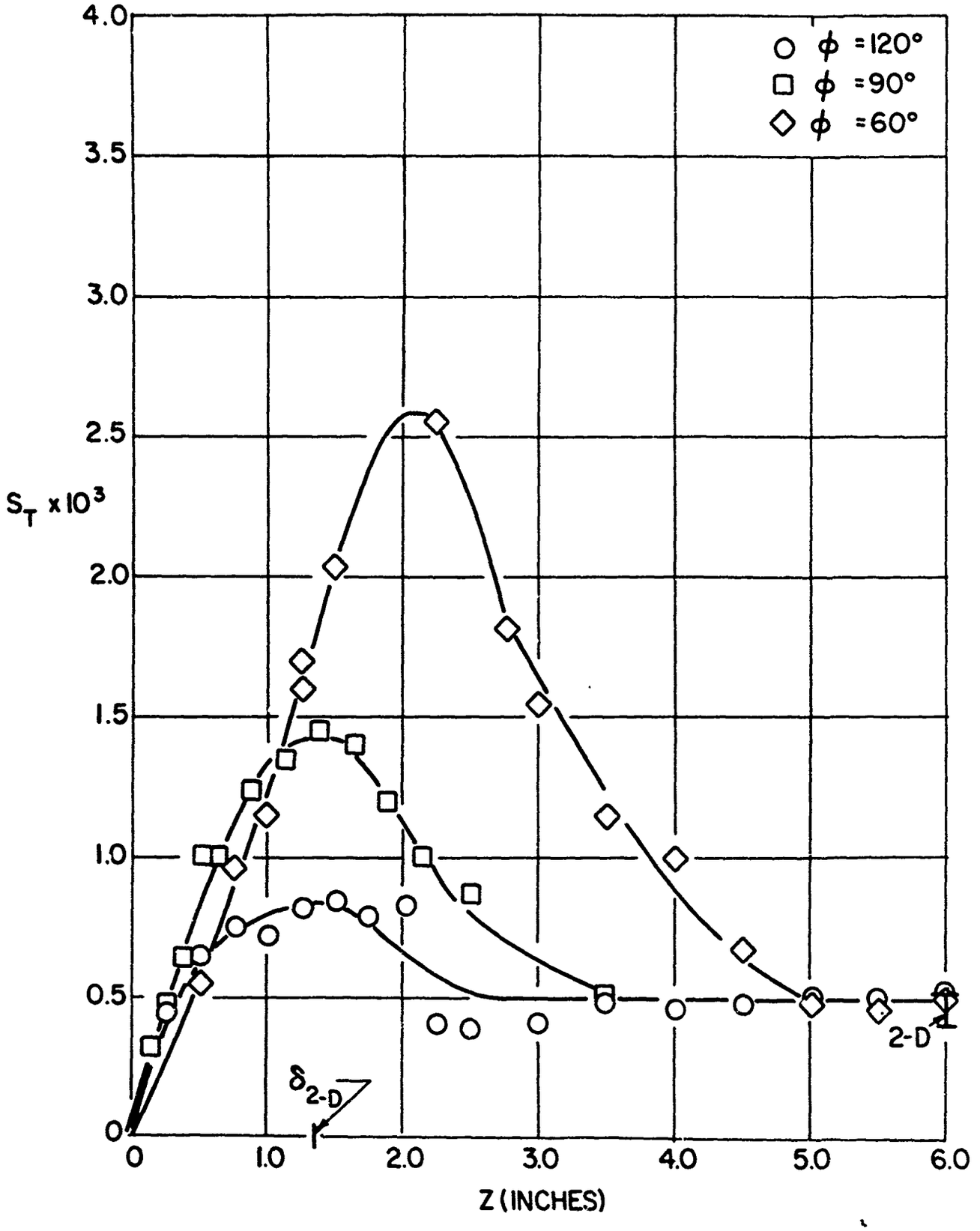

FIG. (4a) VARIATION OF HEAT TRANSFER WITH CORNER ANGLE – $\bar{X}$=2.5

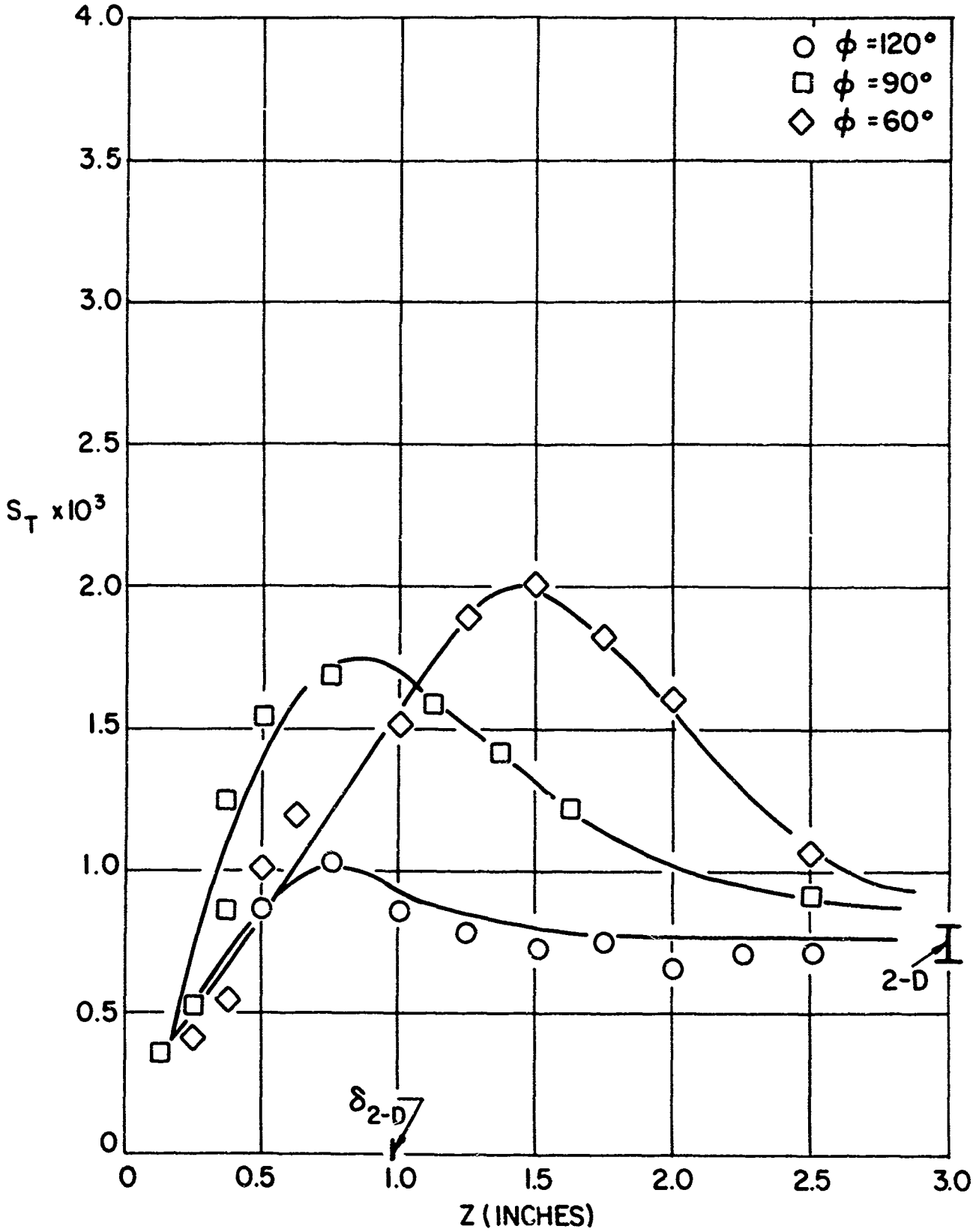

FIG. (4b) VARIATION OF HEAT TRANSFER WITH CORNER ANGLE — $\bar{X} = 3.1$

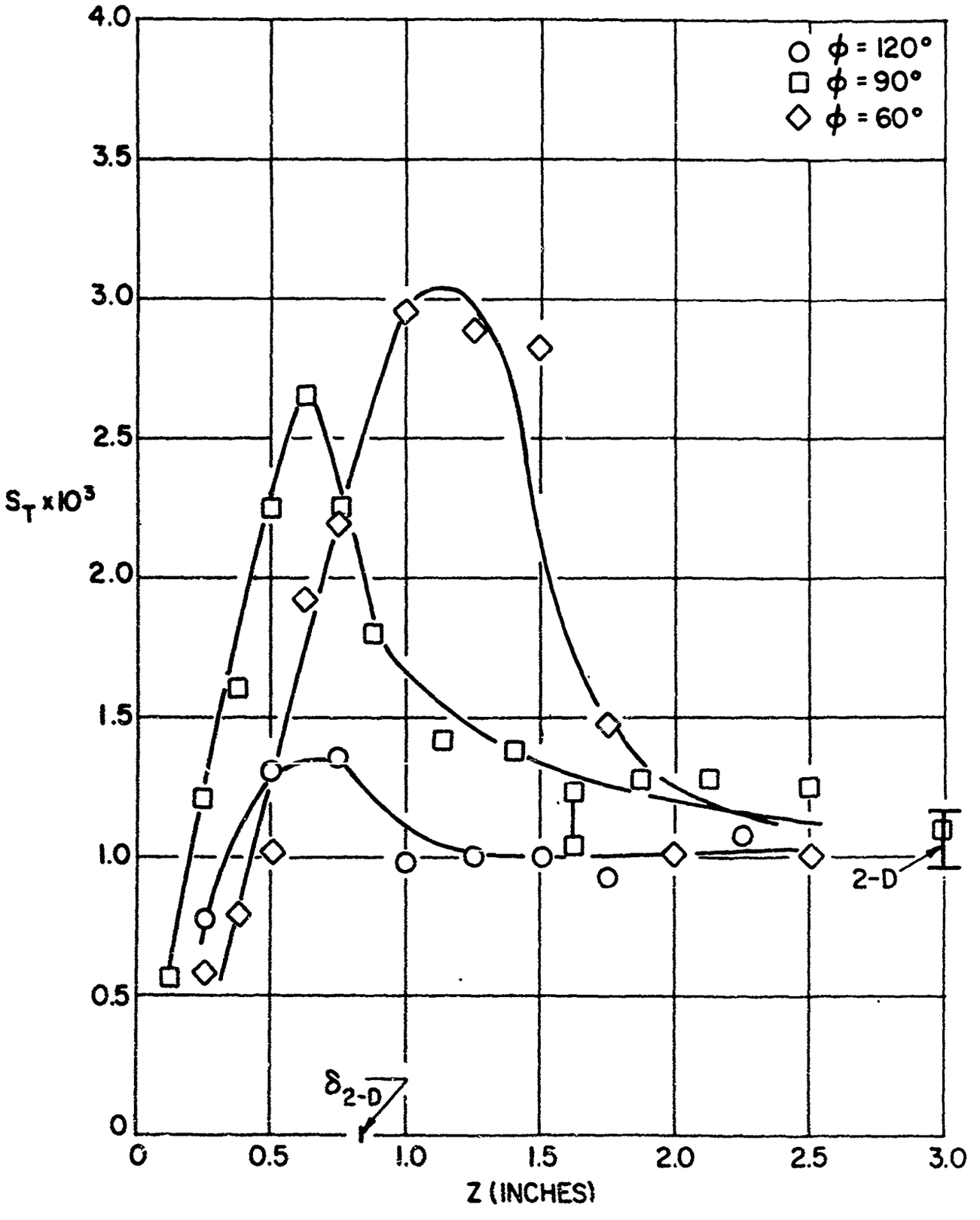

FIG. (4c) VARIATION OF HEAT TRANSFER WITH CORNER ANGLE– $\bar{X} = 4.1$

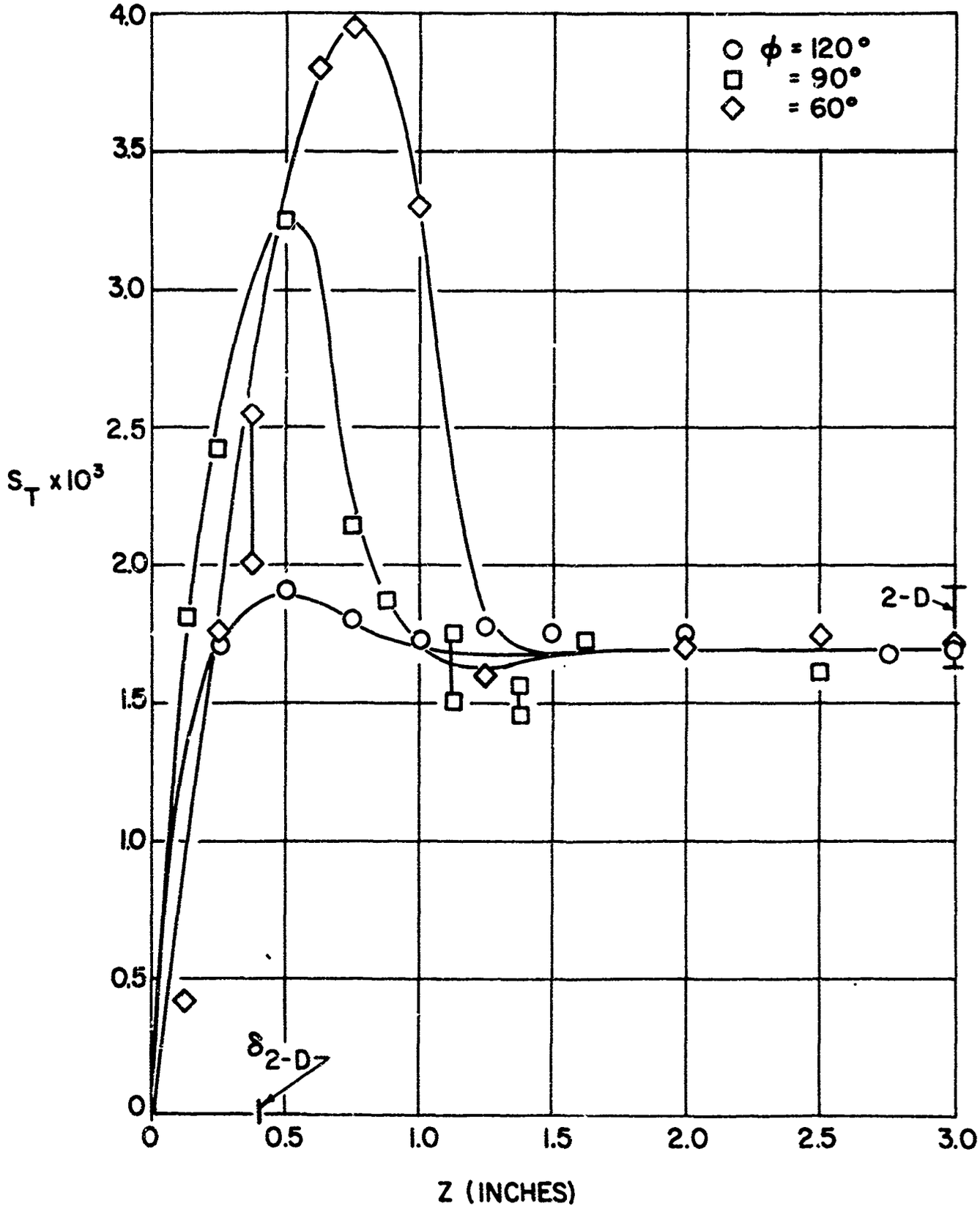

FIG. (4 d) VARIATION OF HEAT TRANSFER WITH CORNER ANGLE — $\bar{X} = 5.6$

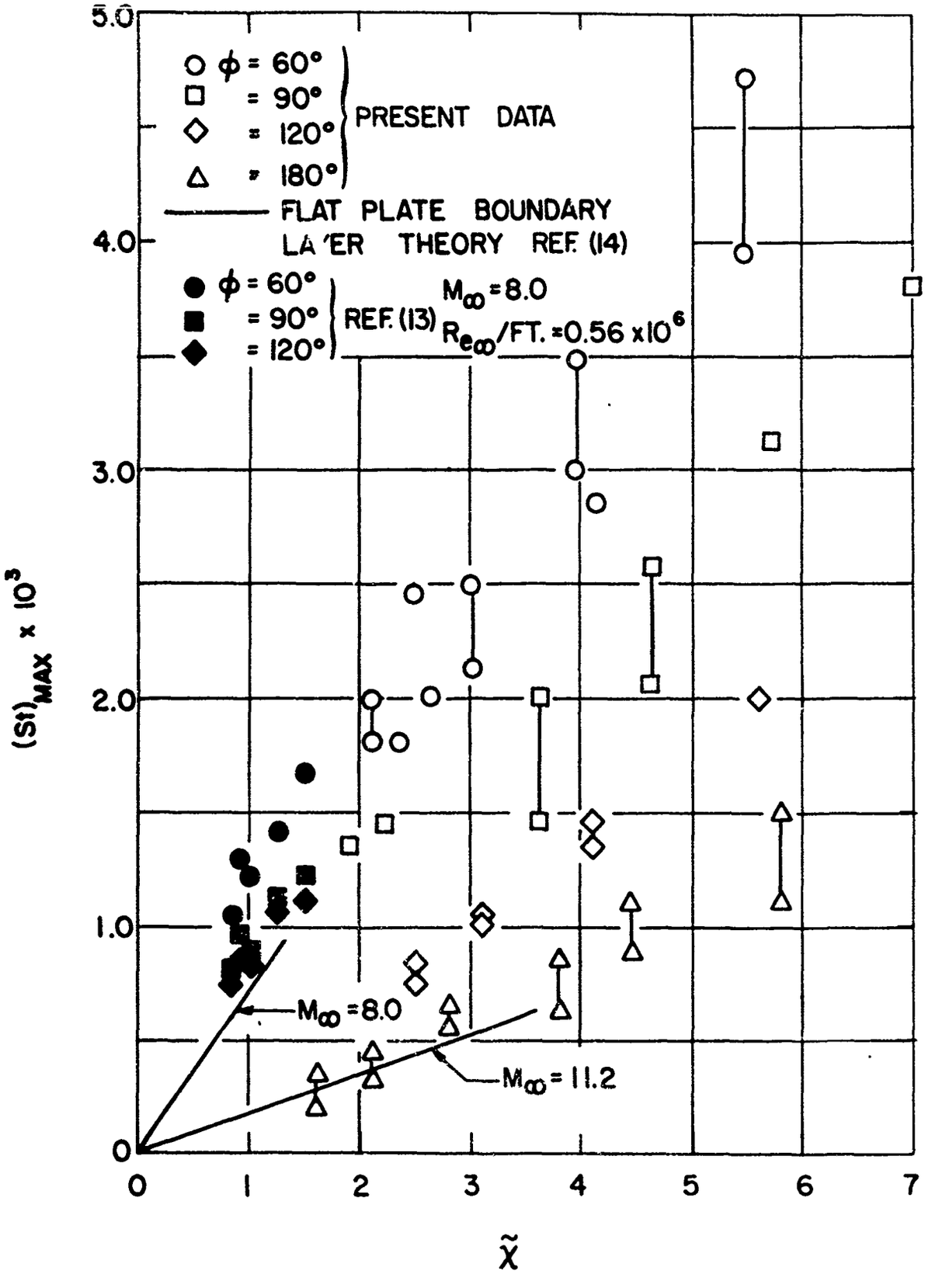

FIG. (5) MAXIMUM HEAT TRANSFER IN CORNER

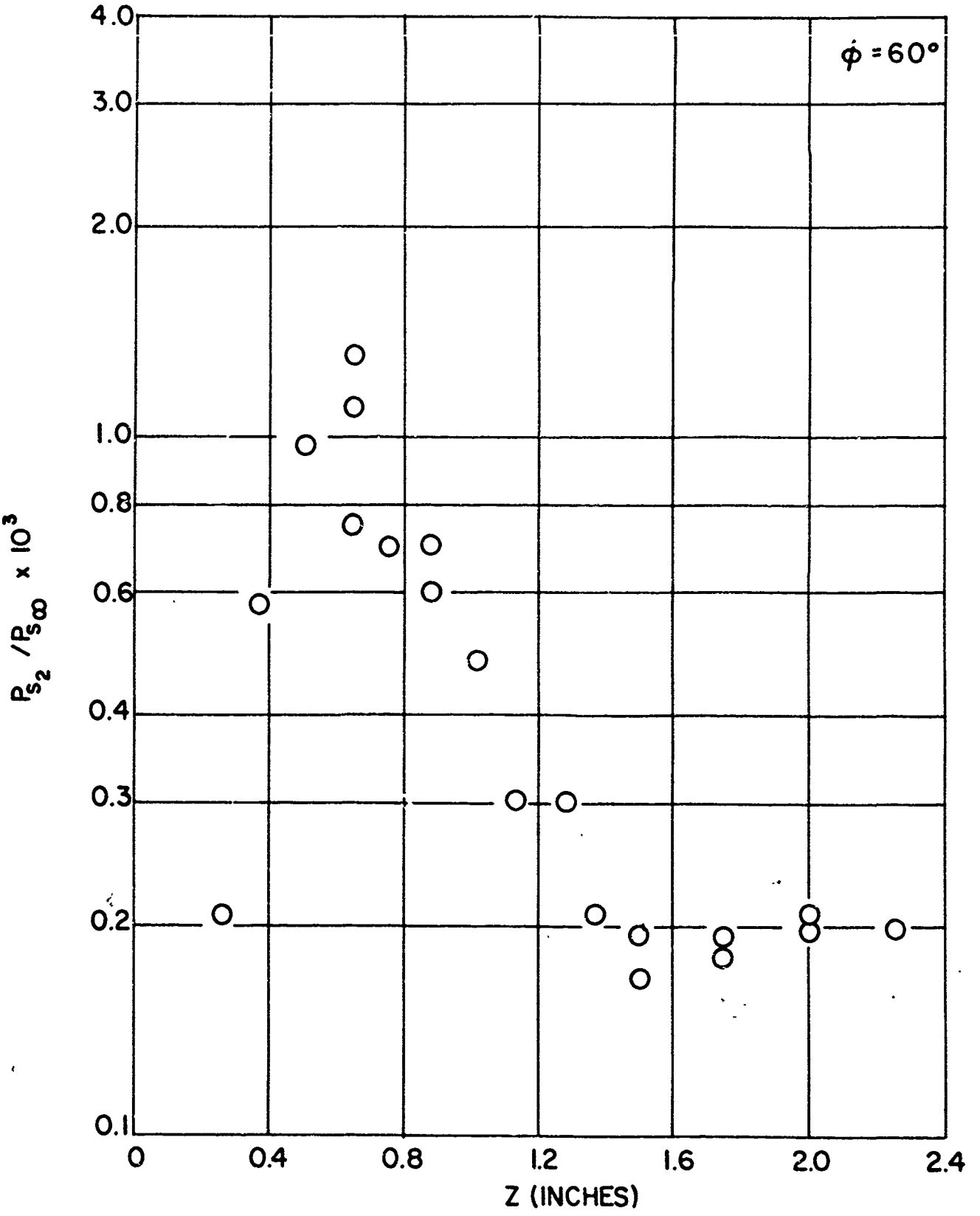

FIG. (6) PITOT PRESSURE PROFILES, $\bar{X} = 5.0$
(a) Y = .25 INCHES

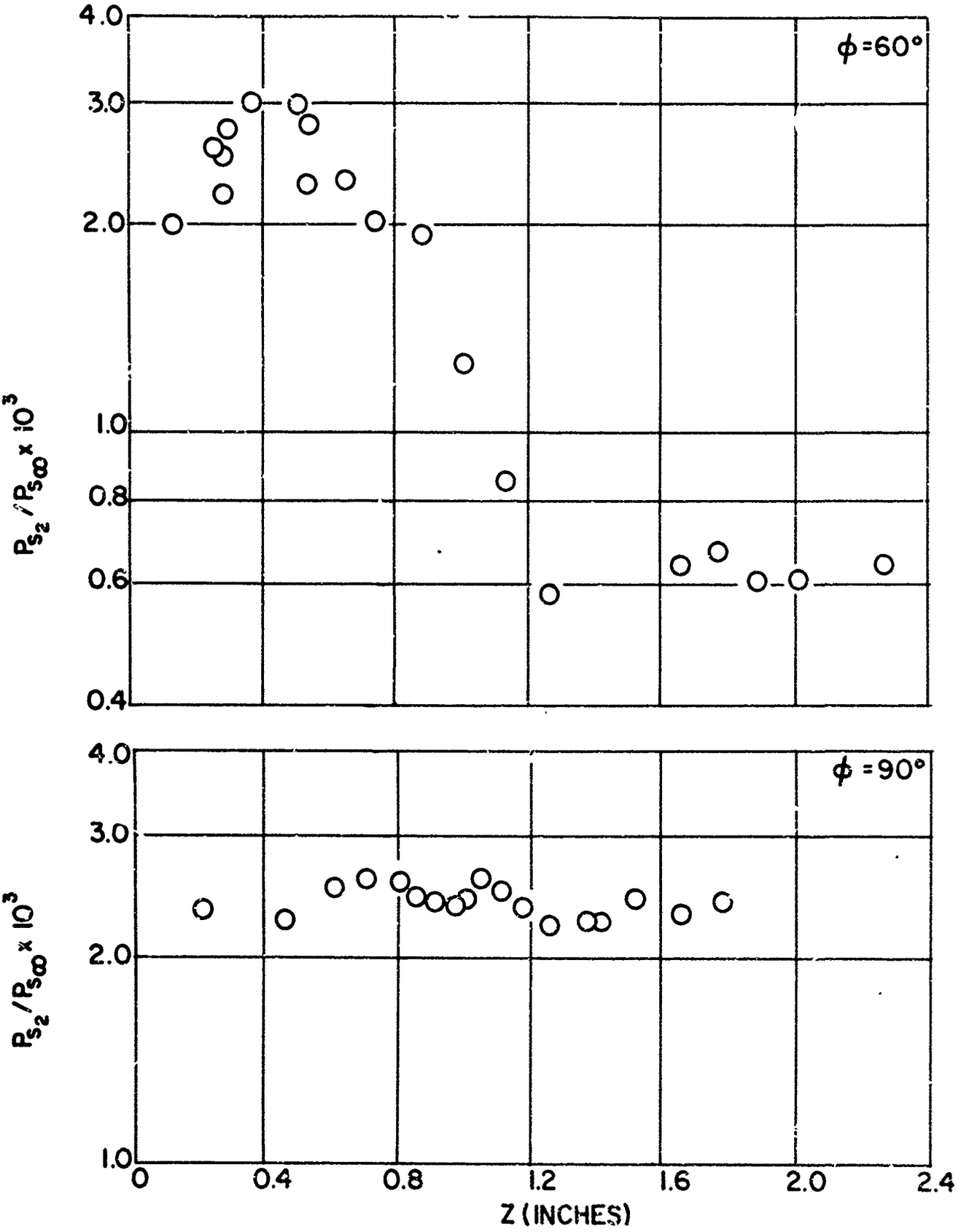

FIG. (6) PITOT PRESSURE PROFILES, $\bar{X}$=5.0
(b) Y ≈ .55 INCHES

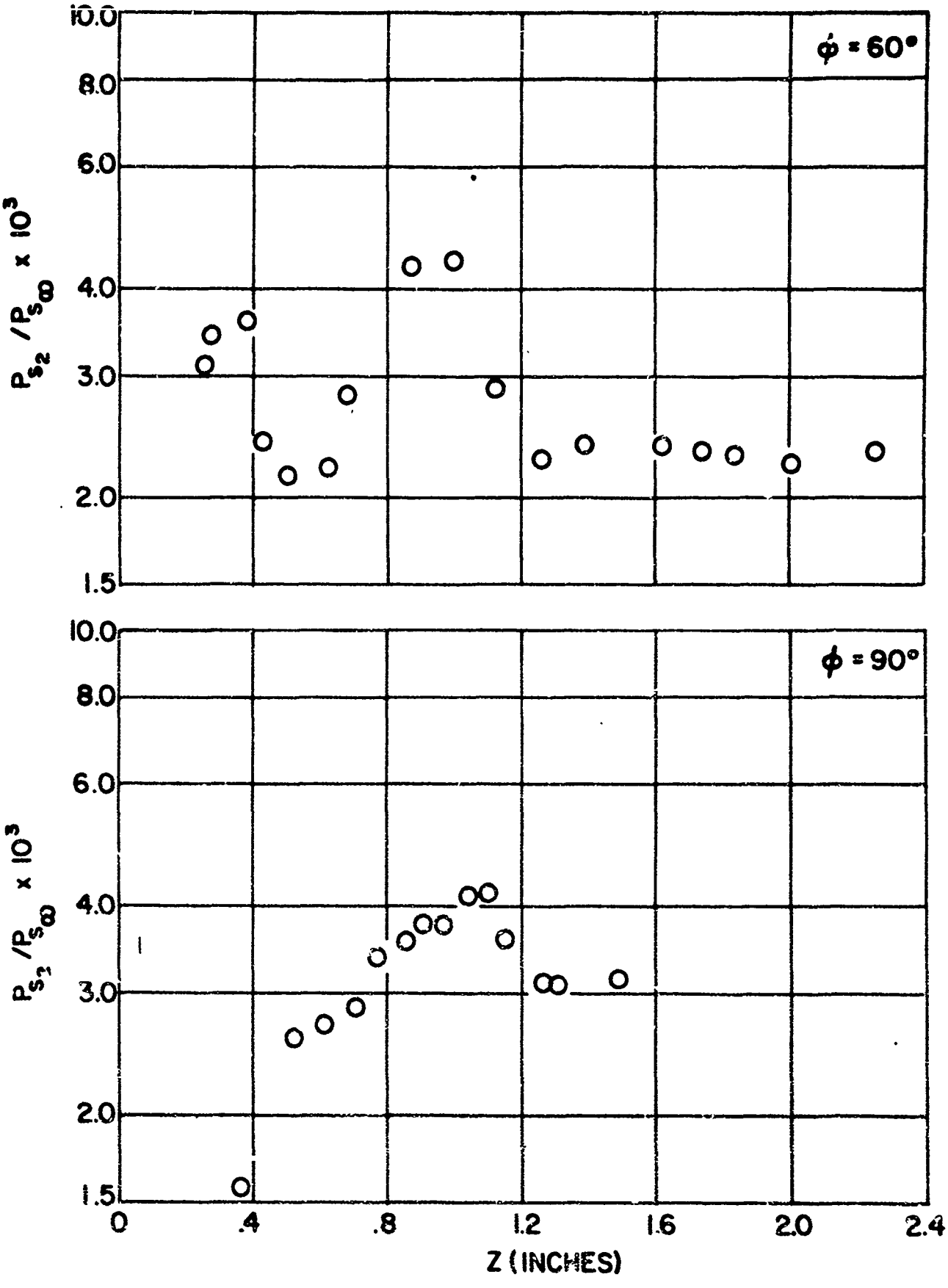

FIG. (6) PITOT PRESSURE PROFILES, $\bar{X} = 5.0$
(c) Y = 0.75 INCHES

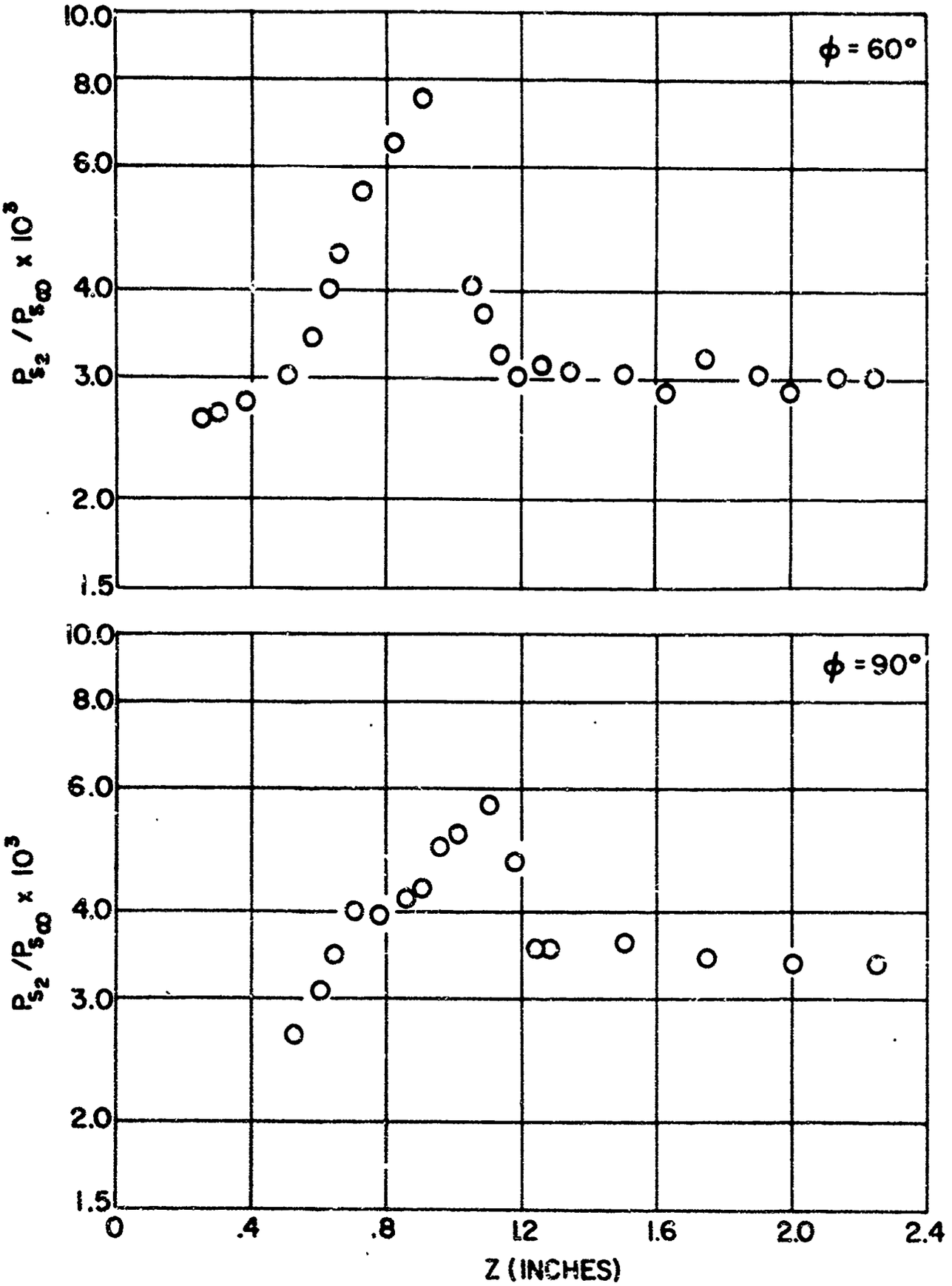

FIG. (6) PITOT PRESSURE PROFILES, $\bar{X} = 5.0$
(d) Y =0.90 INCHES

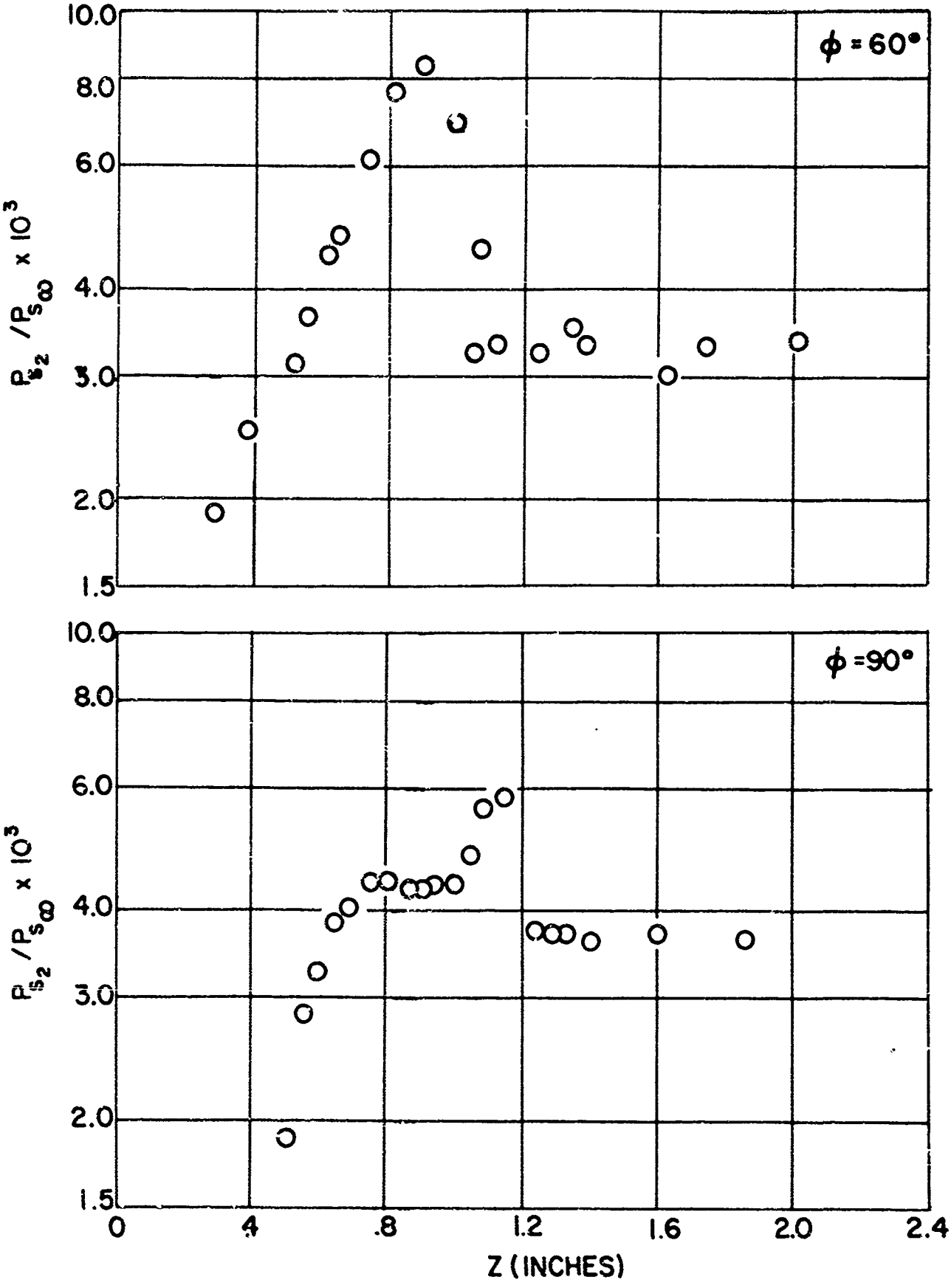

FIG.(6) PITOT PRESSURE PROFILES, $\bar{X}$=5.0
(e) Y = 1.00 INCHES

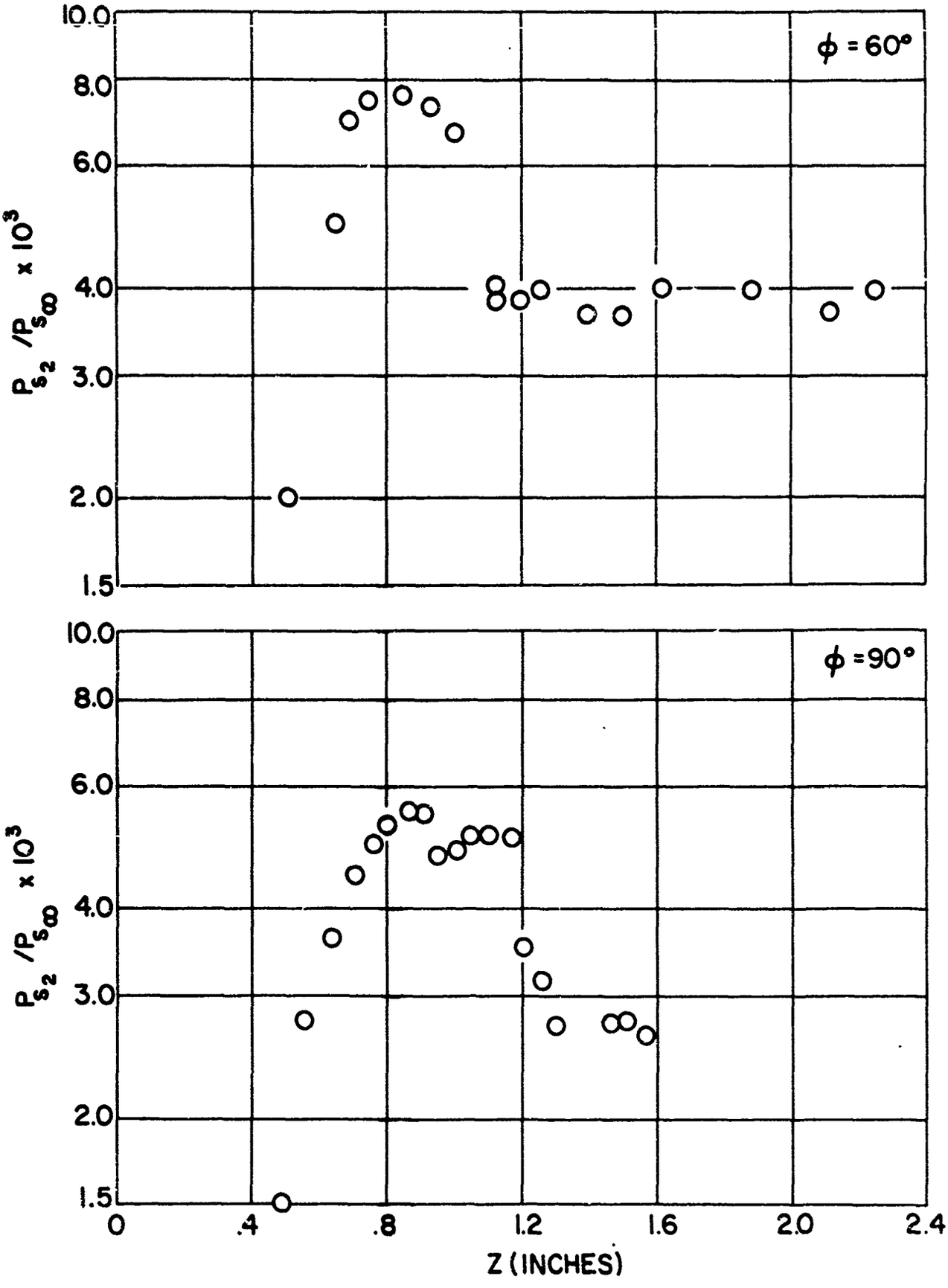

FIG. (6) PITOT PRESSURE PROFILES, $\bar{X} = 5.0$
(f) Y = 1.10 INCHES

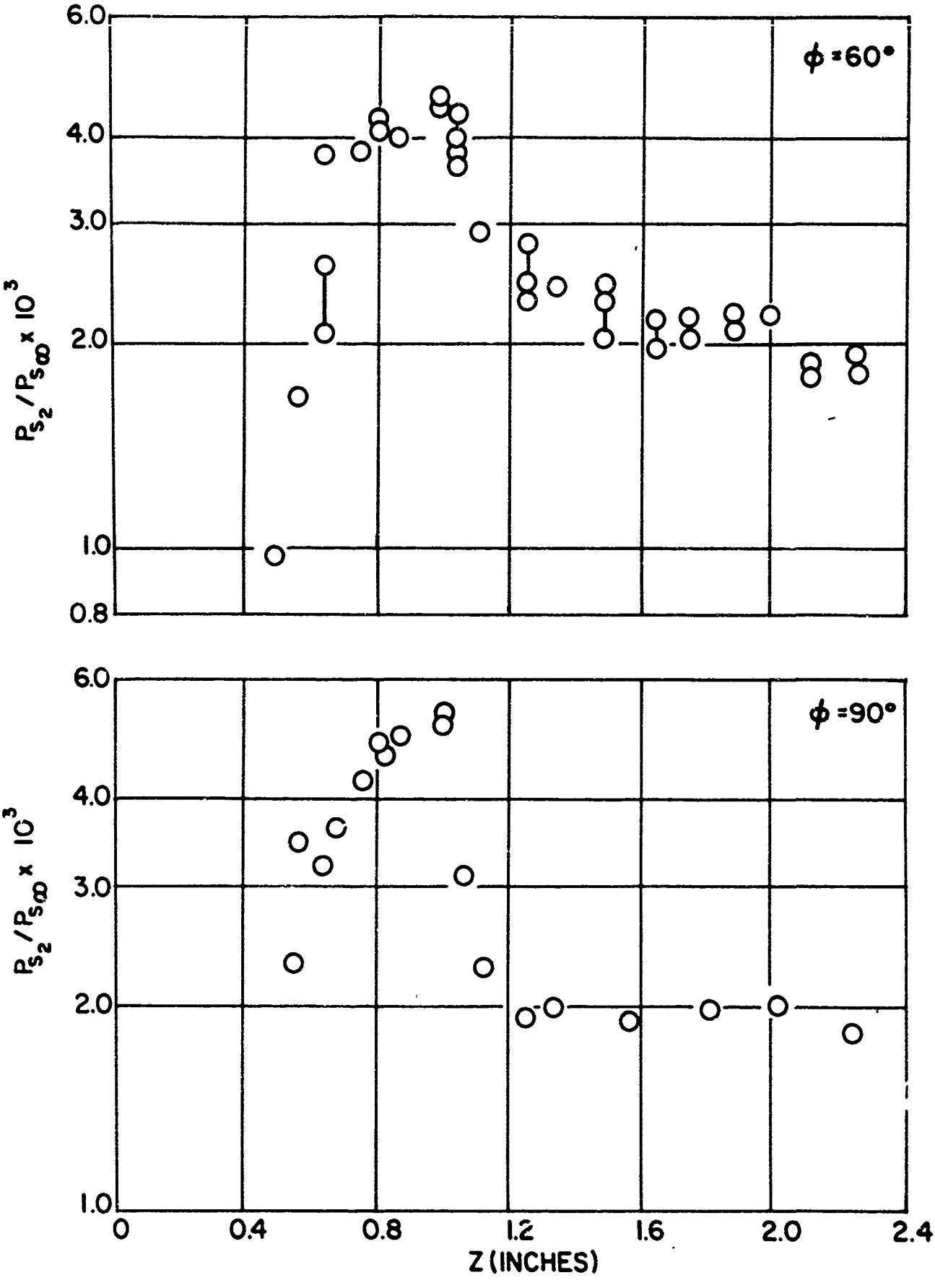

FIG. (6) PITOT PRESSURE PROFILES, $\bar{X} = 5.0$
(g) Y = 1.25 INCHES

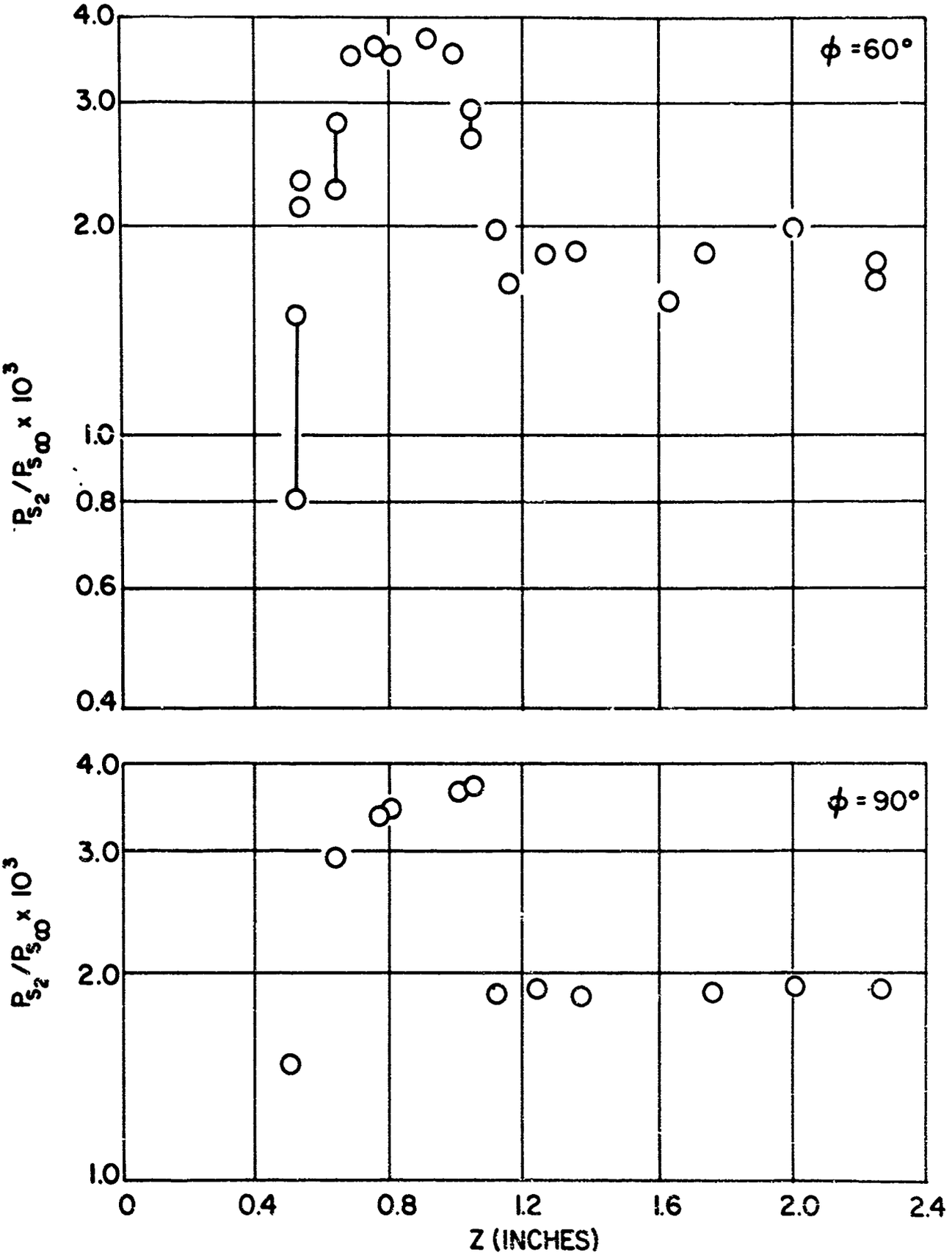

FIG. (6) PITOT PRESSURE PROFILES, $\bar{X} = 5.0$
(h) Y = 1.50 INCHES

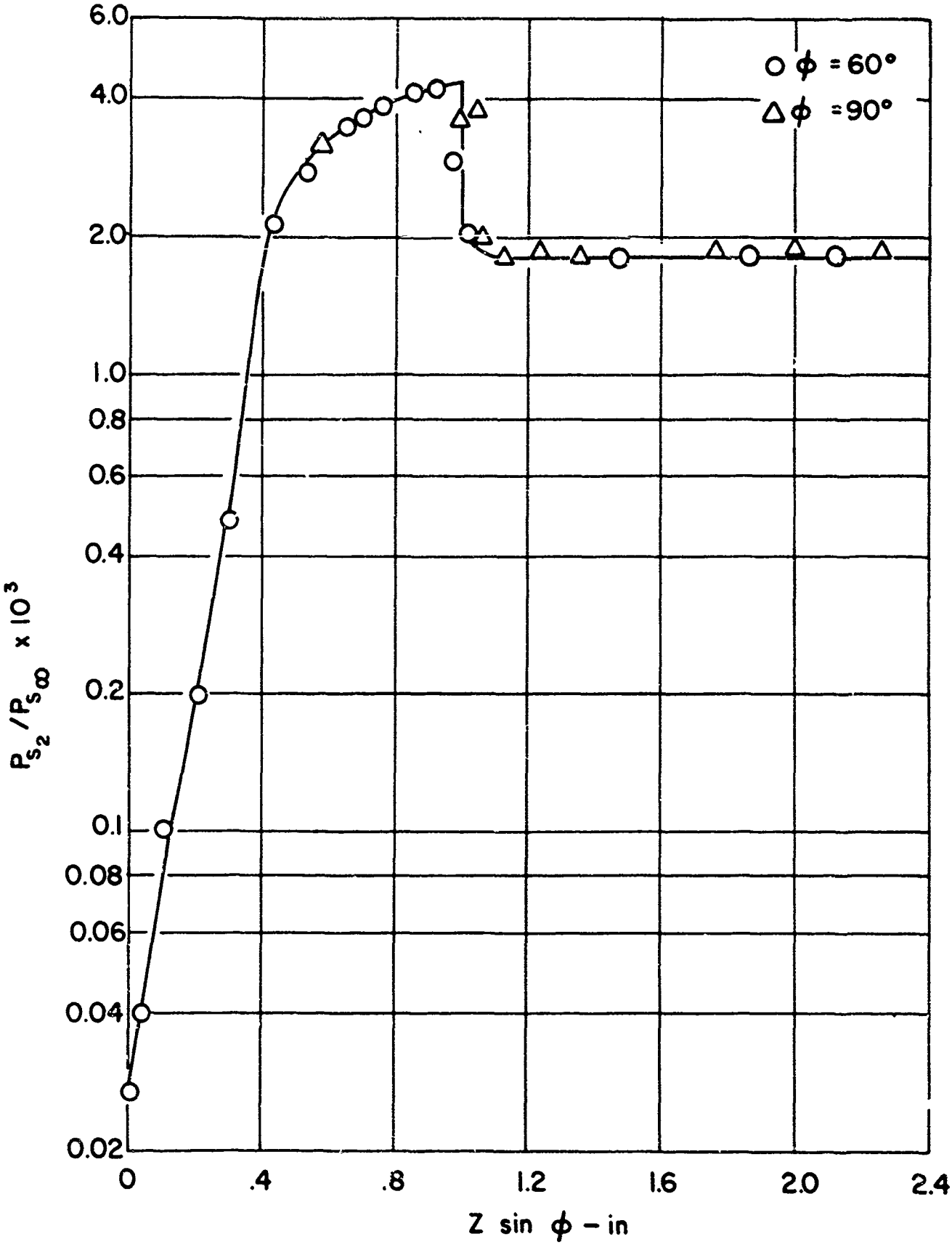

FIG. (6) PITOT PRESSURE PROFILES, $\bar{X} = 5.0$
(i) TWO DIMENSIONAL ($Y \to \infty$)

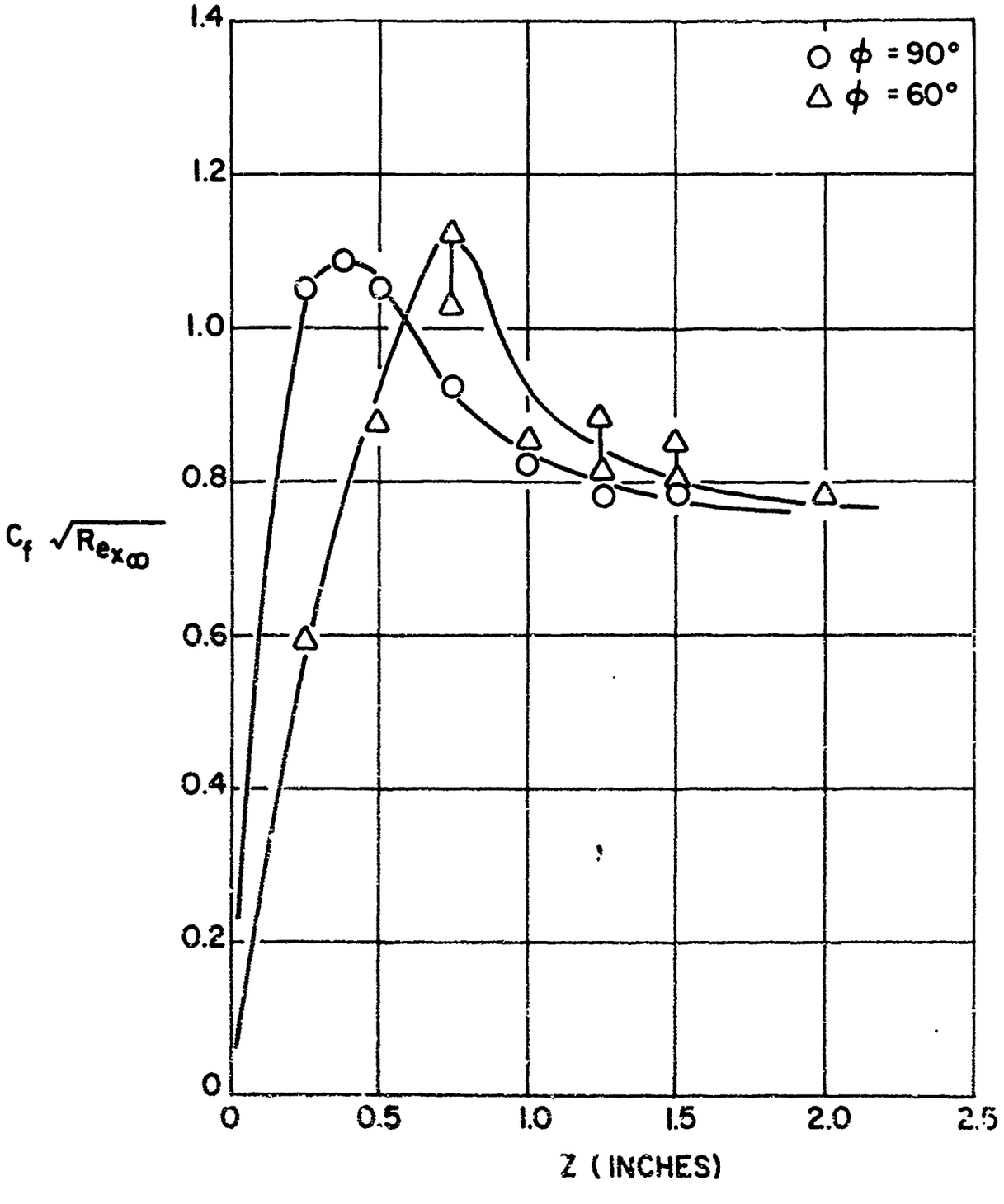

FIG. (7) VARIATION OF SKIN FRICTION WITH CORNER ANGLE, $\bar{X}$ = 5.0

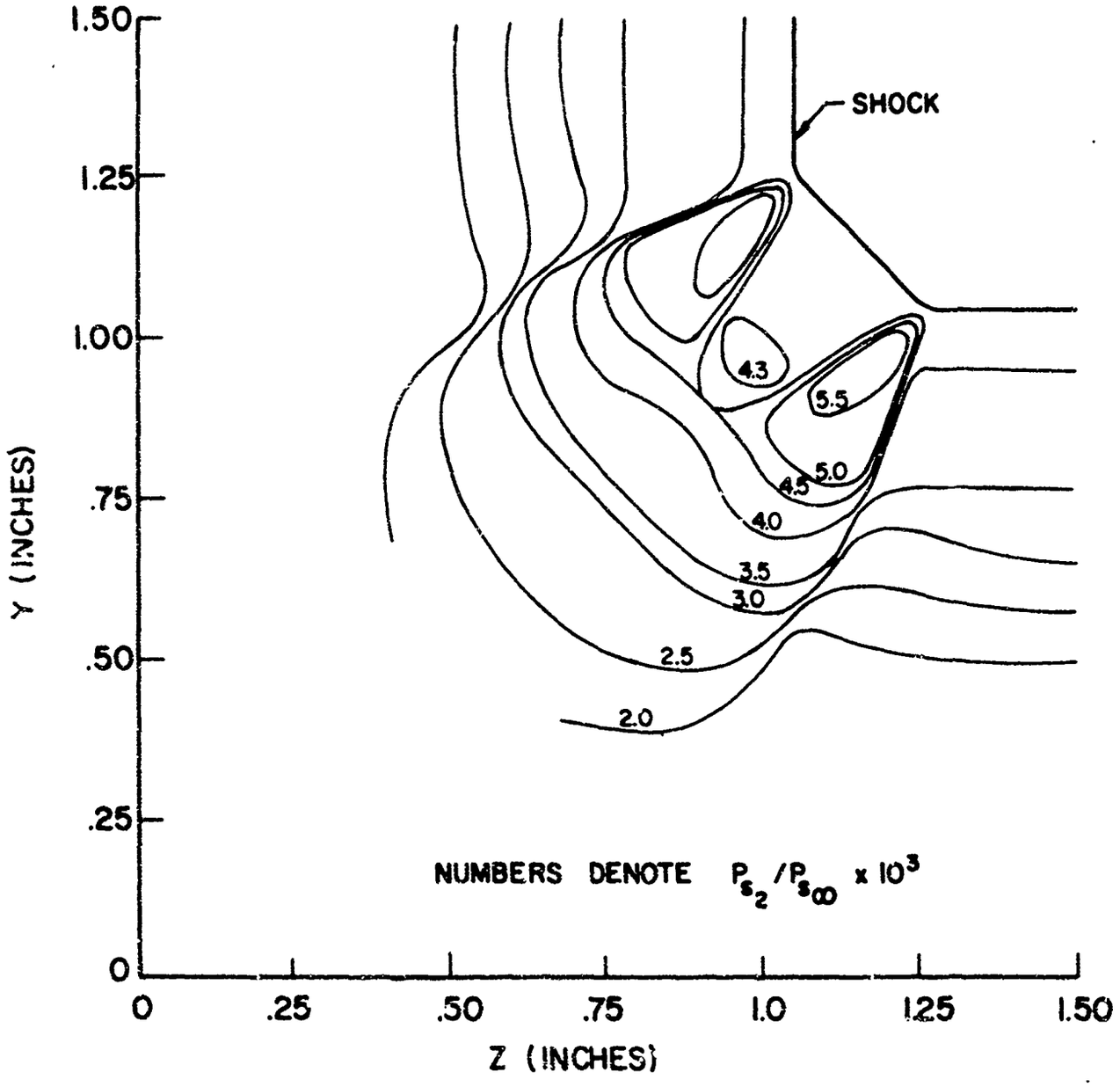

FIG.(8) PITOT CONTOURS IN CORNER – $\bar{X} = 5.0$
(a) $\phi = 90°$

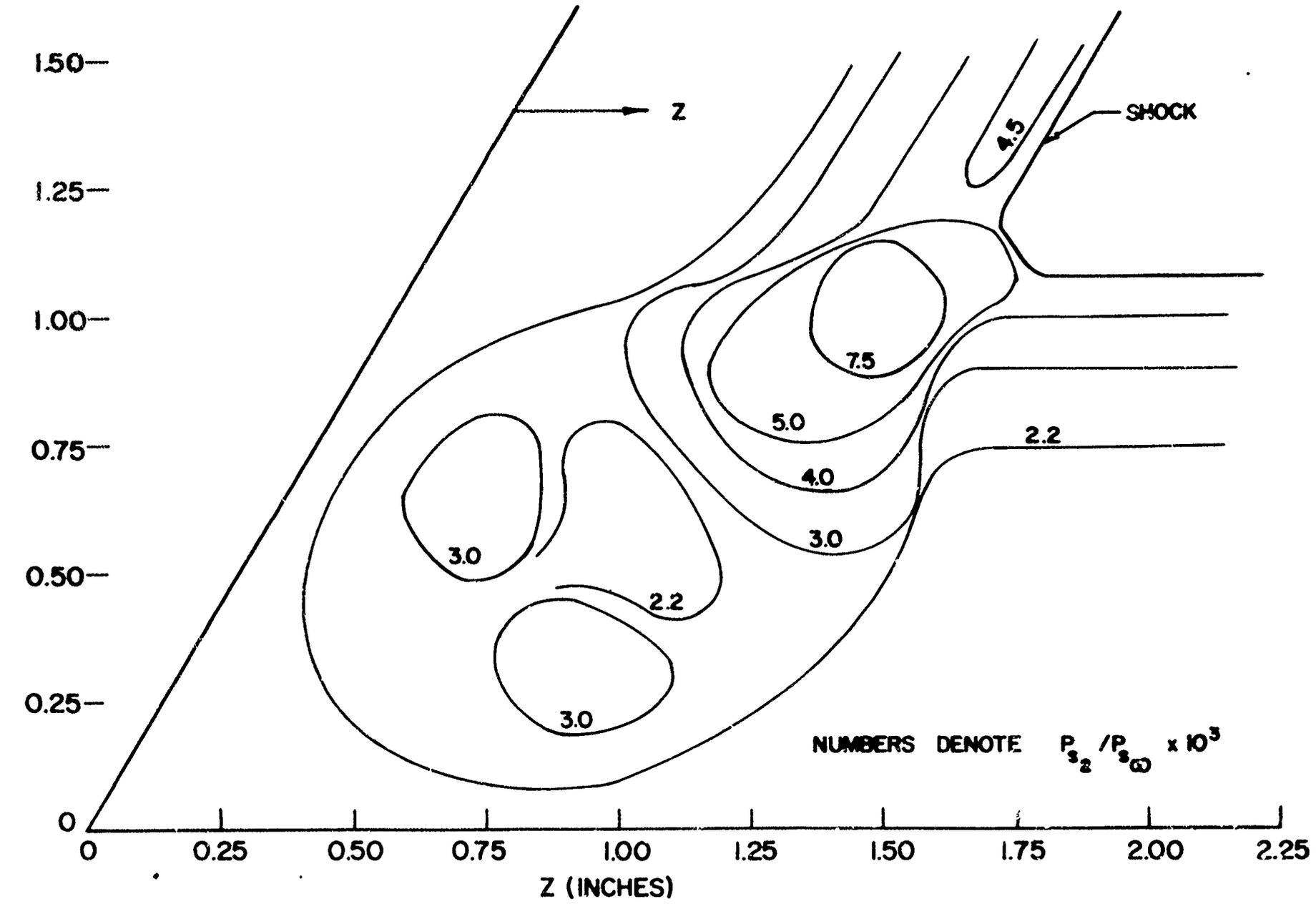

FIG. (8) PITOT CONTOURS IN CORNER – $\bar{X} = 5.0$
(b) $\phi = 60°$

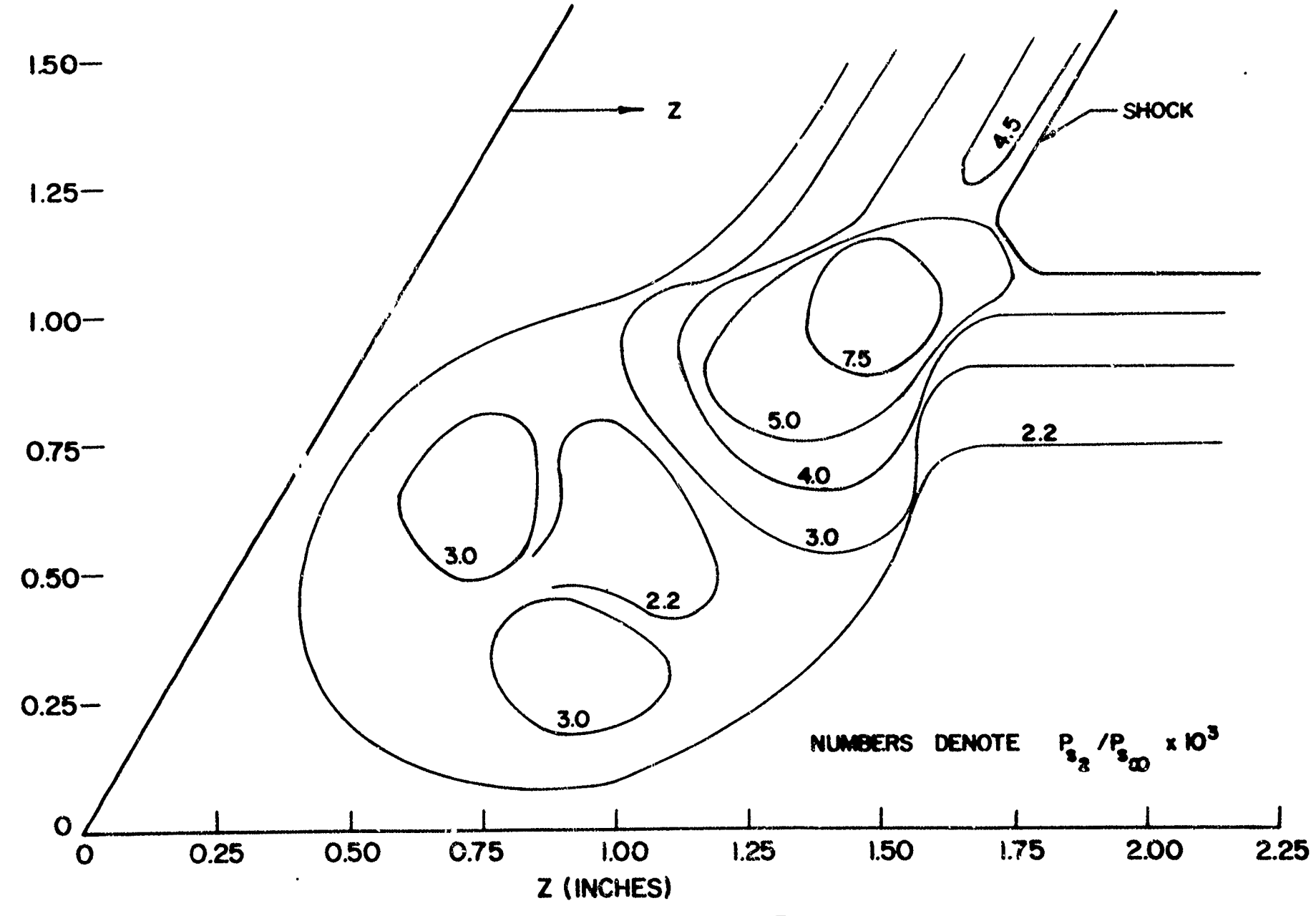

FIG. (8) PITOT CONTOURS IN CORNER – $\bar{X} = 5.0$
(b) $\phi = 60°$

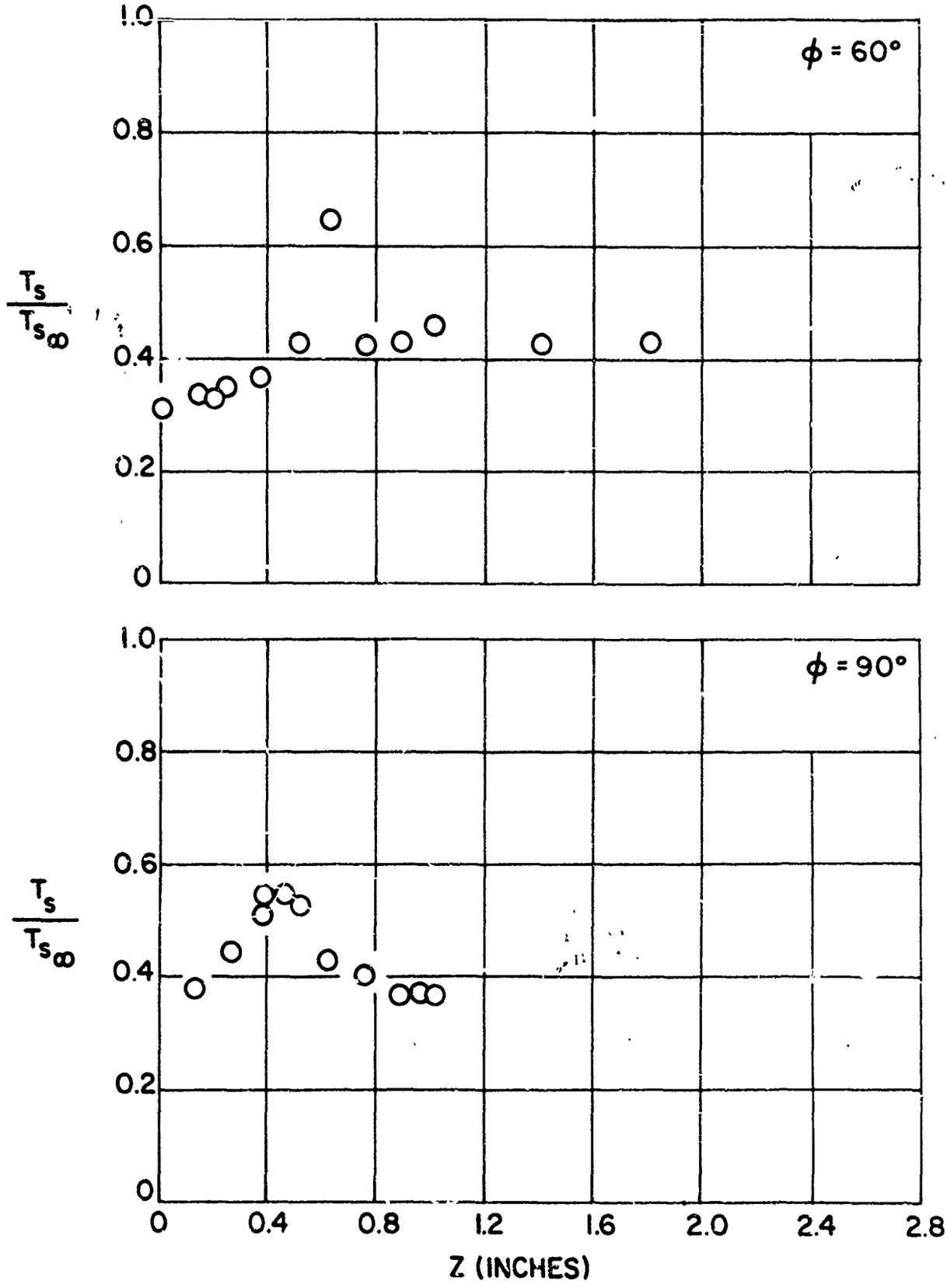

FIG. (9) STAGNATION TEMPERATURE PROFILES, $\bar{X} = 5.0$
(a) Y = .125 INCHES

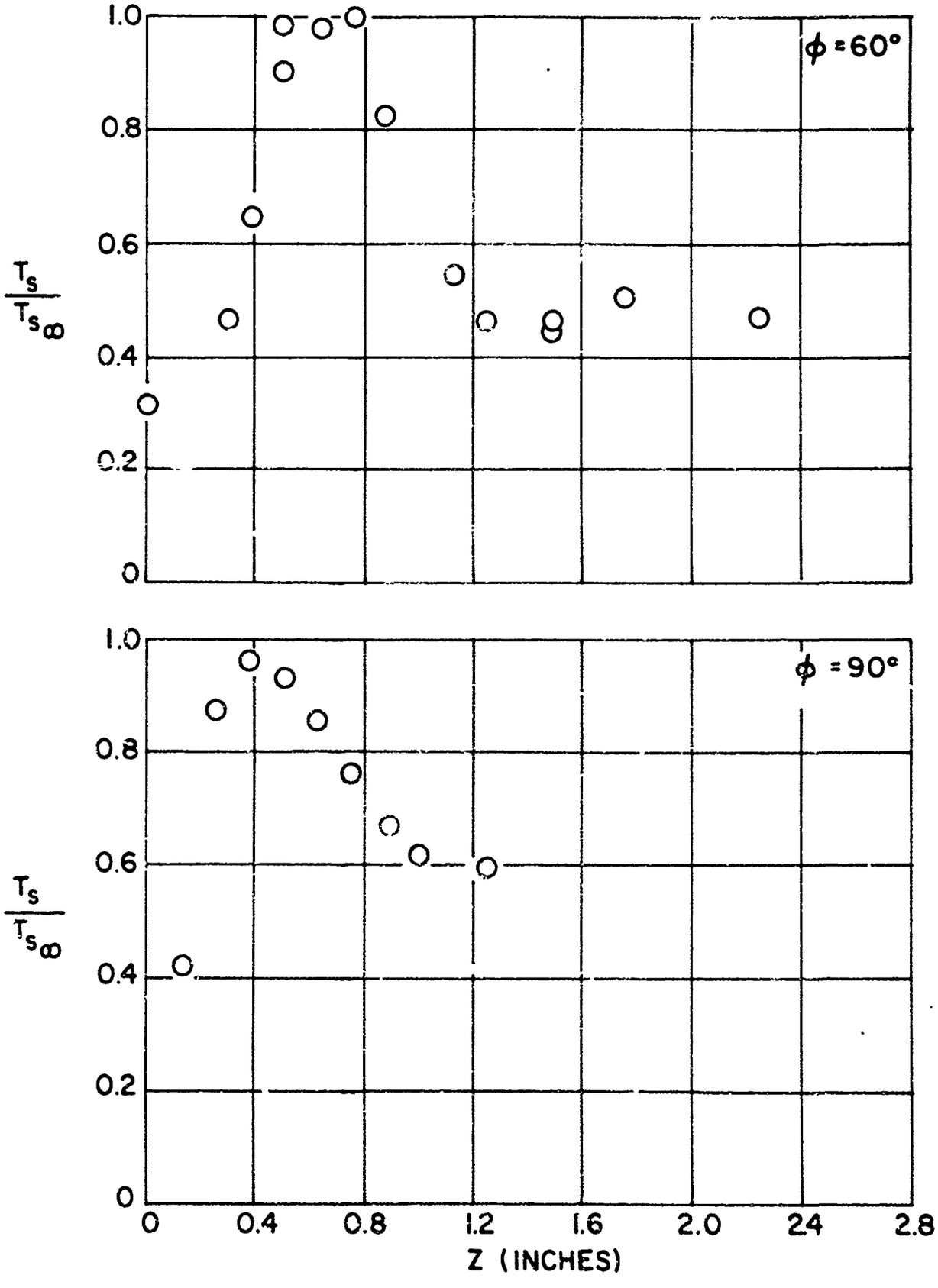

FIG. (9) STAGNATION TEMPERATURE PROFILES, $\bar{X} = 5.0$
(b) Y = 0.25 INCHES

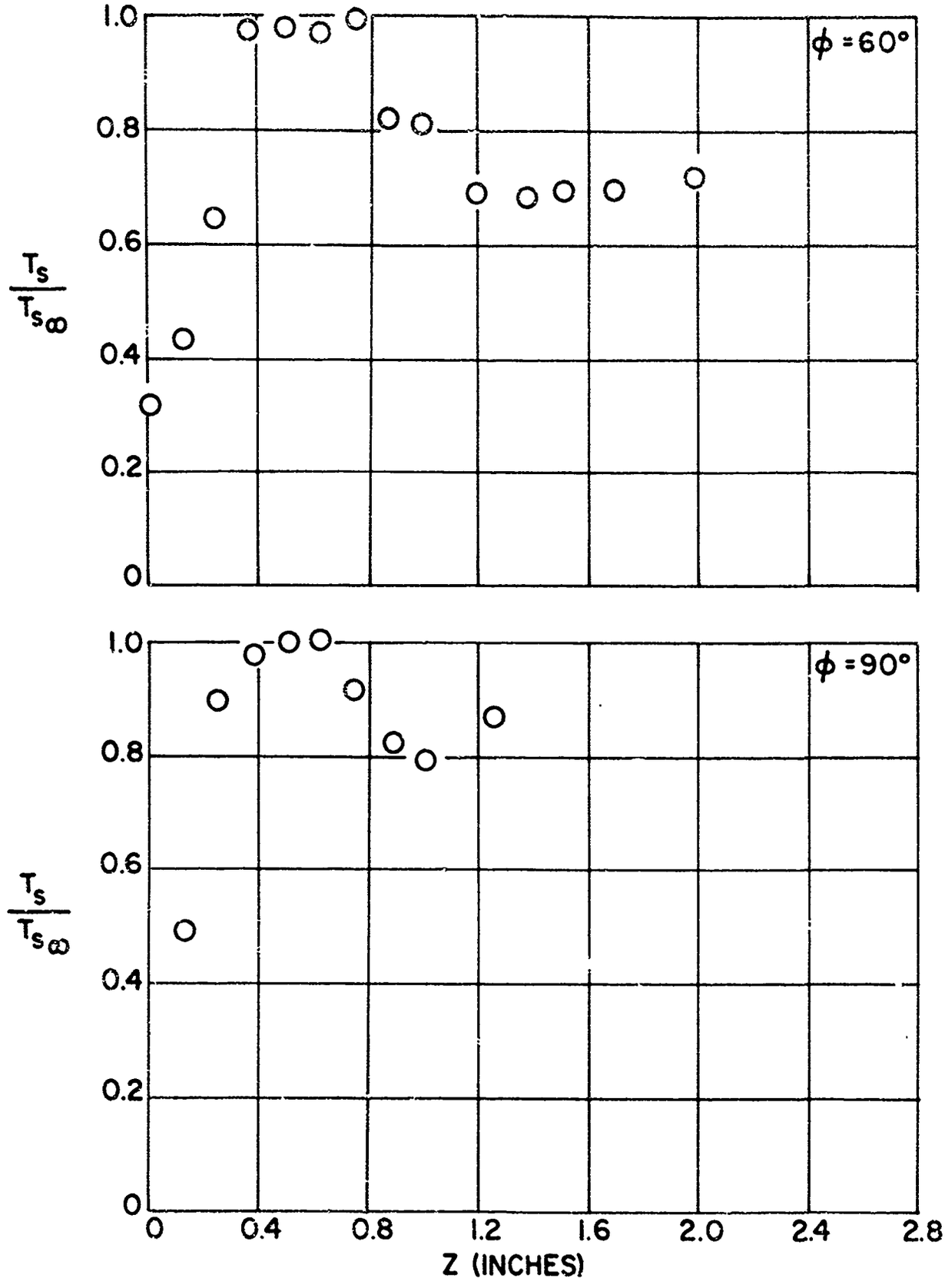

FIG. (9) STAGNATION TEMPERATURE PROFILES, $\bar{X} = 5.0$
(c) $Y = 0.375$ INCHES

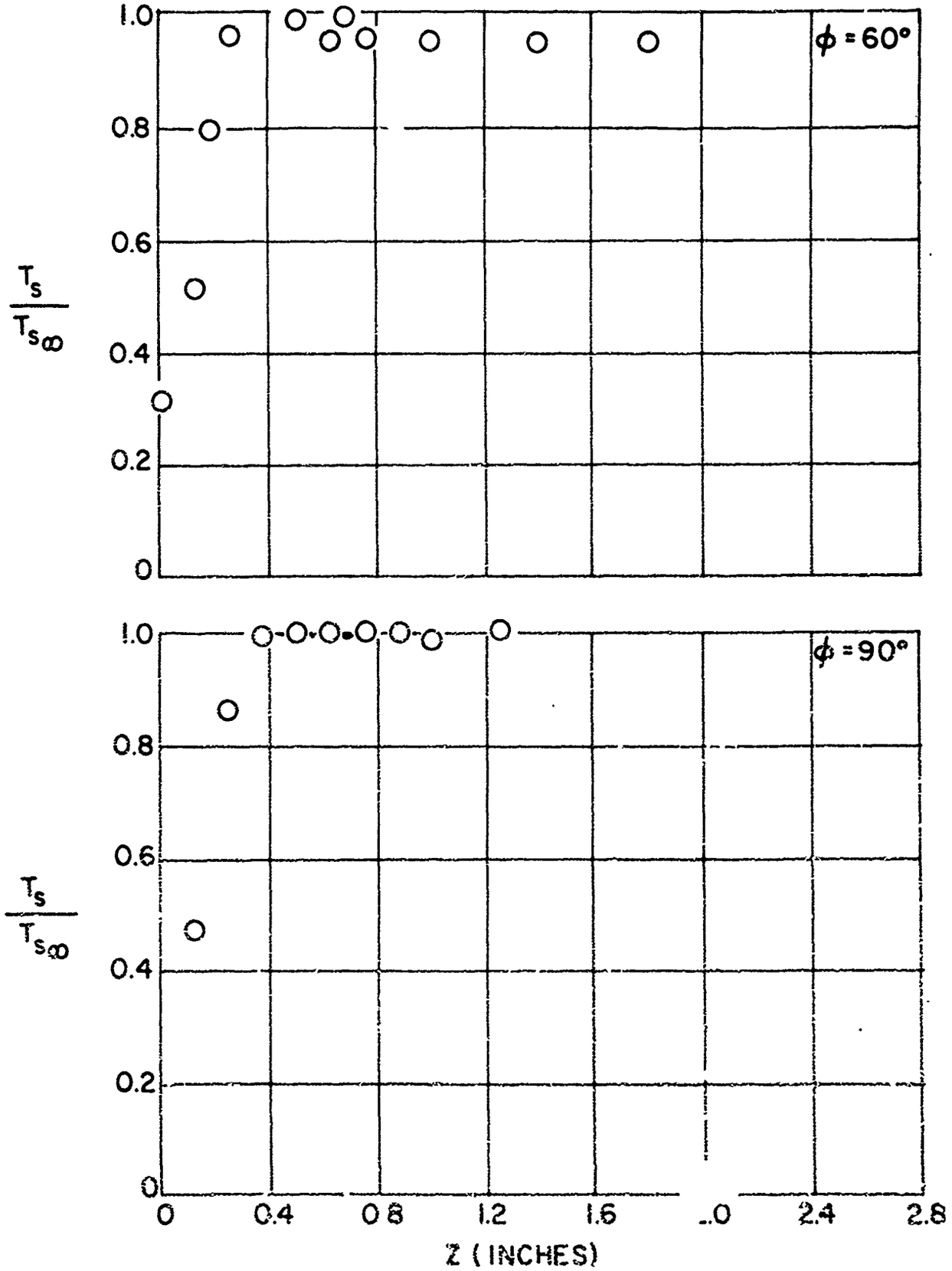

FIG. (9) STAGNATION TEMPERATURE PROFILES, $\bar{X}$=5.0
(d) Y=0.50 INCHES

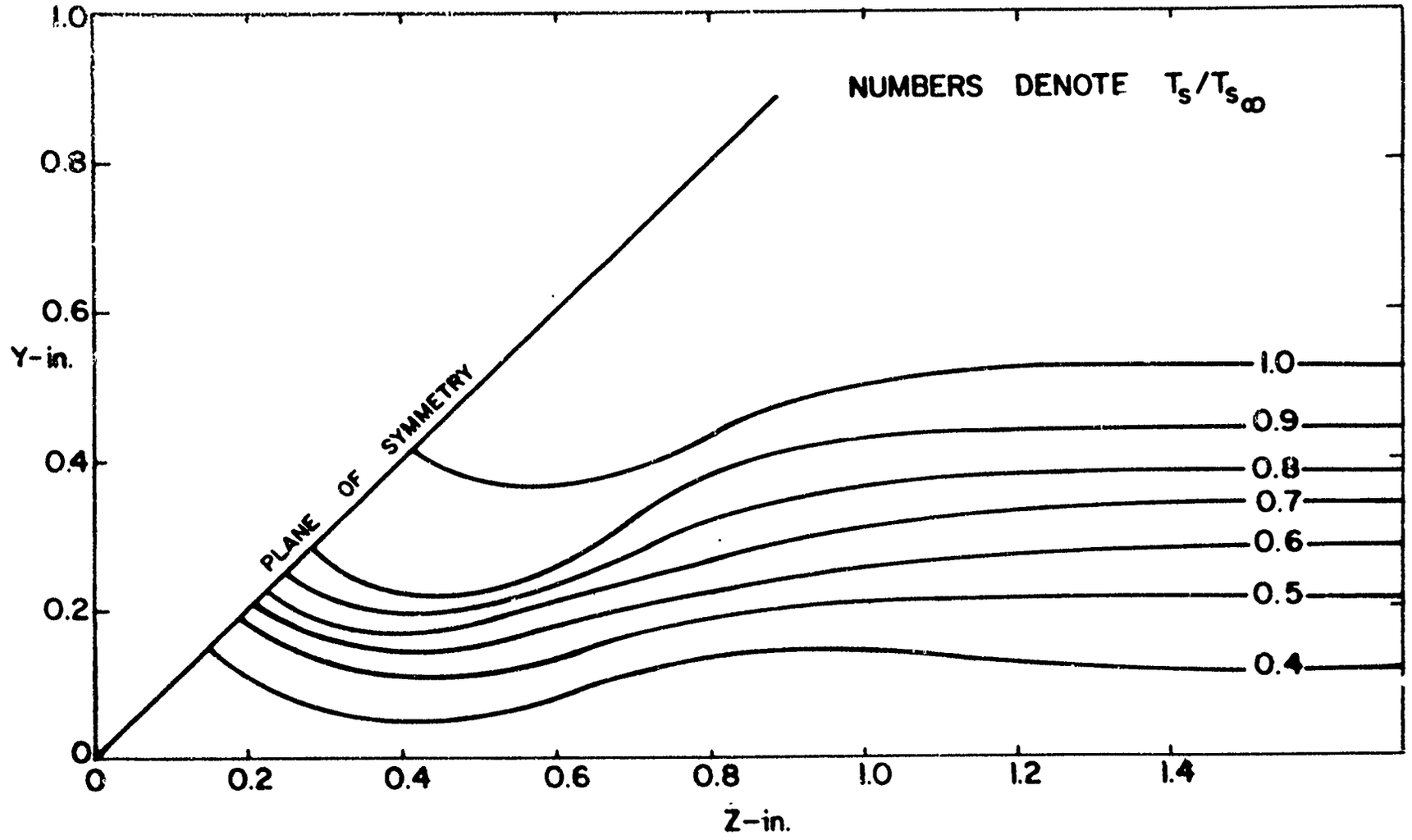

FIG. (10) STAGNATION TEMPERATURE CONTOURS IN CORNER REGION, $\bar{X} = 5.0$
(a) $\phi = 90°$

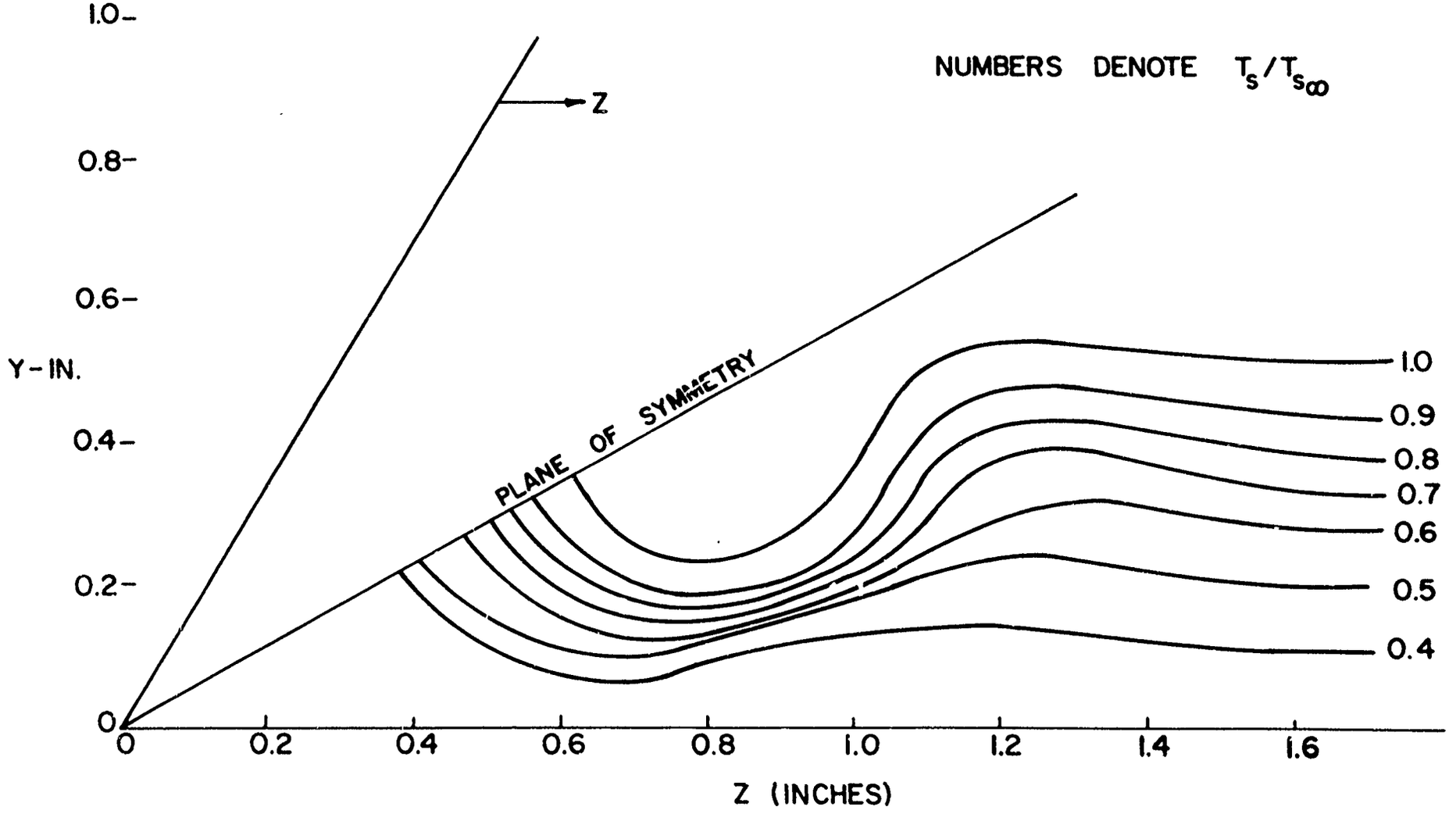

FIG. (10) STAGNATION TEMPERATURE CONTOURS IN CORNER REGION, $\bar{X} = 5.0$
(b) $\phi = 60°$

Unclassified
Security Classification

DOCUMENT CONTROL DATA - R & D

(Security classification of title, body of abstract and indexing annotation must be entered when the overall report is classified)

1. ORIGINATING ACTIVITY (Corporate author) Polytechnic Institute of Brooklyn Graduate Center Route 110, Farmingdale, New York 11735	2a. REPORT SECURITY CLASSIFICATION Unclassified 2b. GROUP

3. REPORT TITLE

EXPERIMENTAL MEASUREMENTS OF HYPERSONIC CORNER FLOW

4. DESCRIPTIVE NOTES (Type of report and inclusive dates)

Scientific Interim

5. AUTHOR(S) (First name, middle initial, last name)

Charles T. Nardo
Robert J. Cresci

6. REPORT DATE	7a. TOTAL NO. OF PAGES	7b. NO. OF REFS
January 1969	42	14

8a. CONTRACT OR GRANT NO.	9a. ORIGINATOR'S REPORT NUMBER(S)
AF 49(638)-1623 b. PROJECT NO 9781-01 c. 6144501F d. 681307	PIBAL Report No. 69-1 9b. OTHER REPORT NO(S) (Any other numbers that may be assigned this report) AFOSR 69-1228TR

10. DISTRIBUTION STATEMENT

1. This document has been approved for public release and sale; its distribution is unlimited.

11. SUPPLEMENTARY NOTES	12. SPONSORING MILITARY ACTIVITY
TECH, OTHER	AF Office of Scientific Research (SREM) 1400 Wilson Boulevard Arlington, Virginia 22209

13. ABSTRACT

An experimental investigation has been conducted of the viscous-inviscid interaction occurring along the interior corner of two intersecting flat plates under hypersonic, low density, conditions.

The program involves the measurement of surface heat transfer rates and surface pressures in the vicinity of a corner with included angles of 60°, 90° and 120°. The interpretation of these measurements gives rise to some understanding of local flow behavior and, therefore, on the nature of the three-dimensional boundary layer and shock shape within the corner region. In addition, pitot and temperature surveys are conducted in cross planes to obtain information pertaining to the flow field variables within the corner region, and also, the complex shock configuration which extends into the viscous layer. This data is presented on contour maps in order to facilitate easier visual interpretation.

The test program was conducted in the Mach 11.2, blowdown wind tunnel of the Polytechnic Institute of Brooklyn, Gas Dynamics Laboratory. Test Reynolds numbers of 1.5×10^4/in were obtained in this facility and a constant wall to free stream stagnation temperature ratio of 0.32 was maintained throughout the investigation.

DD FORM 1 NOV 65 1473

Unclassified
Security Classification

Unclassified
Security Classification

DOCUMENT CONTROL DATA - R & D

(Security classification of title, body of abstract and indexing annotation must be entered when the overall report is classified)

ORIGINATING ACTIVITY (Corporate author)
Polytechnic Institute of Brooklyn
Graduate Center
Route 110, Farmingdale, New York 11735

2a. REPORT SECURITY CLASSIFICATION
Unclassified

2b. GROUP

REPORT TITLE
EXPERIMENTAL MEASUREMENTS OF HYPERSONIC CORNER FLOW

DESCRIPTIVE NOTES (Type of report and inclusive dates)
Scientific Interim

AUTHOR(S) (First name, middle initial, last name)
Charles T. Nardo
Robert J. Cresci

REPORT DATE	7a. TOTAL NO OF PAGES	7b. NO. OF REFS
January 1969	42	14

CONTRACT OR GRANT NO	9a. ORIGINATOR'S REPORT NUMBER(S)
AF 49(638)-1623	PIBAL Report No. 69-1
PROJECT NO 9781-01 6144501F 681307	9b. OTHER REPORT NO(S) (Any other numbers that may be assigned this report) AFOSR 69-1228TR

DISTRIBUTION STATEMENT
1. This document has been approved for public release and sale; its distribution is unlimited.

SUPPLEMENTARY NOTES	12 SPONSORING MILITARY ACTIVITY
TECH, OTHER	AF Office of Scientific Research (SREM) 1400 Wilson Boulevard Arlington, Virginia 22209

ABSTRACT

An experimental investigation has been conducted of the viscous-inviscid interaction occurring along the interior corner of two intersecting flat plates under hypersonic, low density, conditions.

The program involves the measurement of surface heat transfer rates and surface pressures in the vicinity of a corner with included angles of 60°, 90° and 120°. The interpretation of these measurements gives rise to some understanding of local flow behavior and, therefore, on the nature of the three-dimensional boundary layer and shock shape within the corner region. In addition, pitot and temperature surveys are conducted in cross planes to obtain information pertaining to the flow field variables within the corner region, and also, the complex shock configuration which extends into the viscous layer. This data is presented on contour maps in order to facilitate easier visual interpretation.

The test program was conducted in the Mach 11.2, blowdown wind tunnel of the Polytechnic Institute of Brooklyn, Gas Dynamics Laboratory. Test Reynolds numbers of 1.5×10^4/in were obtained in this facility and a constant wall to free stream stagnation temperature ratio of 0.32 was maintained throughout the investigation.

DD FORM 1 NOV 65 1473

Unclassified
Security Classification